Title

Notch expression during ctenophore development gives insight into its ancestral function

Authors

*Brent Foster[1], Fredrik Hugosson[1], Cezar Borba[1], James Strother[1], Mark Q. Martindale[1]

Affiliations

1. The Whitney Laboratory for Marine Bioscience, Department of Biology, University of Florida, St. Augustine, FL 32080, USA

* Corresponding author: bf400@exeter.ac.uk

Summary

The canonical *Notch* pathway is a juxtacrine signaling module with widely conserved roles maintaining progenitor cell populations, promoting binary cell fate decisions, and establishing tissue boundaries. This pathway emerged in Metazoan lineages, although many molecular components and regulators existed prior to that divergence. Given that the vast majority of *Notch* studies focus on bilaterians, it is unclear when or how *Notch* gained its developmental signaling functions. To clarify the ancestral function of *Notch*, we turned to an early branching Metazoan — the ctenophore *Mnemiopsis leidyi* — and conducted structural analyses of putative *Notch* components to evaluate predicted signaling potential. We characterized gene expression of these components with *in situ* hybridization and show they are expressed during late embryogenesis. Using hybridization chain reaction (HCR™), we examine *MlNotch* expression relative to canonical transcriptional targets and putative stem cell markers and identify differential expression patterns at a cellular resolution. Pharmacological inhibition reveals zones of active and inactive *MlNotch* during late embryonic development. Our results suggest that *Notch* evolved its signaling potential by the Metazoan divergence and is likely involved in regulating progenitor cell populations and coordinating developmental fate decisions.

Keywords

Notch, molecular evolution, ctenophores

31 **Introduction**

32 The canonical *Notch* pathway is a juxtacrine signaling module involved in various aspects of development
33 across Metazoa. It is best known for its role in promoting binary cell fate decisions via lateral inhibition
34 and/or induction, maintaining stem and progenitor cell populations, and regulating terminal differentiation
35 (for reviews of the role of *Notch* during development, see [1,2]). Many of the key regulatory enzymes and
36 transcriptional targets for *Notch* signaling predate the divergence of Metazoan lineages, suggesting that
37 this pathway evolved by co-opting molecules from pre-existing signaling modules[3,4] (see also Figure 1A).

38 Canonical *Notch* signaling consists of a transmembrane protein that undergoes several distinct
39 proteolytic cleavages for its activation. In the Golgi apparatus, Furin-like convertase forms a *Notch*
40 heterodimer (S1 cleavage) that translocates to the cell membrane, where it acts as a signal receptor. The
41 *Notch* receptor can then interact with a ligand expressed in a neighboring cell, exposing a second
42 extracellular cleavage site recognized by a membrane-bound metalloprotease (S2 cleavage). This
43 cleavage releases the *Notch* extracellular domain (NECD) from the membrane, allowing it to be taken up
44 by the neighboring signaling cell. Meanwhile, γ-secretase in the signal-receiving cell recognizes a third
45 cleavage site and releases the *Notch* intracellular domain (NICD) from the membrane (S3 cleavage),
46 whereupon it translocates to the nucleus and acts as a co-factor to regulate transcription (see Figure 1B for
47 a detailed cell diagram depicting canonical *Notch* signaling in bilaterians).

48 The canonical *Notch* pathway is likely a Metazoan innovation and is present in virtually all
49 bilaterian model systems, although when and how this signaling module emerged during animal evolution
50 remains a mystery. Genomic evidence in single-celled Eukaryotes suggests that domain shuffling of
51 separate proteins could have led to the formation of Metazoan *Notch*[5,6]. A more recent report has
52 identified a *Notch-like* gene with conserved PFAM domains in their canonical order in the
53 choanoflagellate species *Mylnosiga fluctuans*, although to date no study has identified a non-Metazoan
54 species that encodes both *Notch* receptor and a recognizable activating ligand[7]. The vast majority of
55 *Notch* studies are conducted in bilaterians and have demonstrated a broad conservation of components
56 and functions[4,8–10]. Comparative genomics has shown that *Notch* orthologs and putative pathway

57 components have been identified in each non-bilaterian clades, however, to our knowledge *in situ*
58 characterizations of *Notch* components in non-bilaterians have only been conducted in a handful of
59 sponges[11,12] and cnidarians[13–17]. To better understand how the *Notch* pathway and its various
60 developmental functions evolved, it is necessary to understand the developmental context in which these
61 components are expressed in other early branching Metazoan representatives.

62 Ctenophores, as the likely sister group to all other Metazoans[18–20], can offer key evolutionary
63 insight into how *Notch* signaling and its developmental functions emerged in Metazoans, regardless of
64 whether a canonical pathway is intact or not. *Mnemiopsis leidyi,* the primary subject of this report,
65 encodes at least 16 out of 22 canonical *Notch* pathway components in its genome, with several other
66 components reported to be missing so-called diagnostic domains, raising questions concerning their
67 orthology and role in a functional pathway[18]. Existing data only provide presence or absence information
68 which has led subsequent reports to equate the absence of these canonical *Notch* components and PFAM
69 domains as evidence for the absence of a functional signaling pathway[9,10,18]. To date, no study has
70 analyzed the cellular and developmental context in which putative canonical components are expressed
71 during ctenophore development. We therefore have examined the predicted signaling capacity of *M. leidyi*
72 *Notch* (*MlNotch*) and the spatiotemporal expression of putative pathway regulators and targets during
73 early ctenophore development to gain insight into how these components may have evolved to form a
74 functional developmental signaling module.

Results

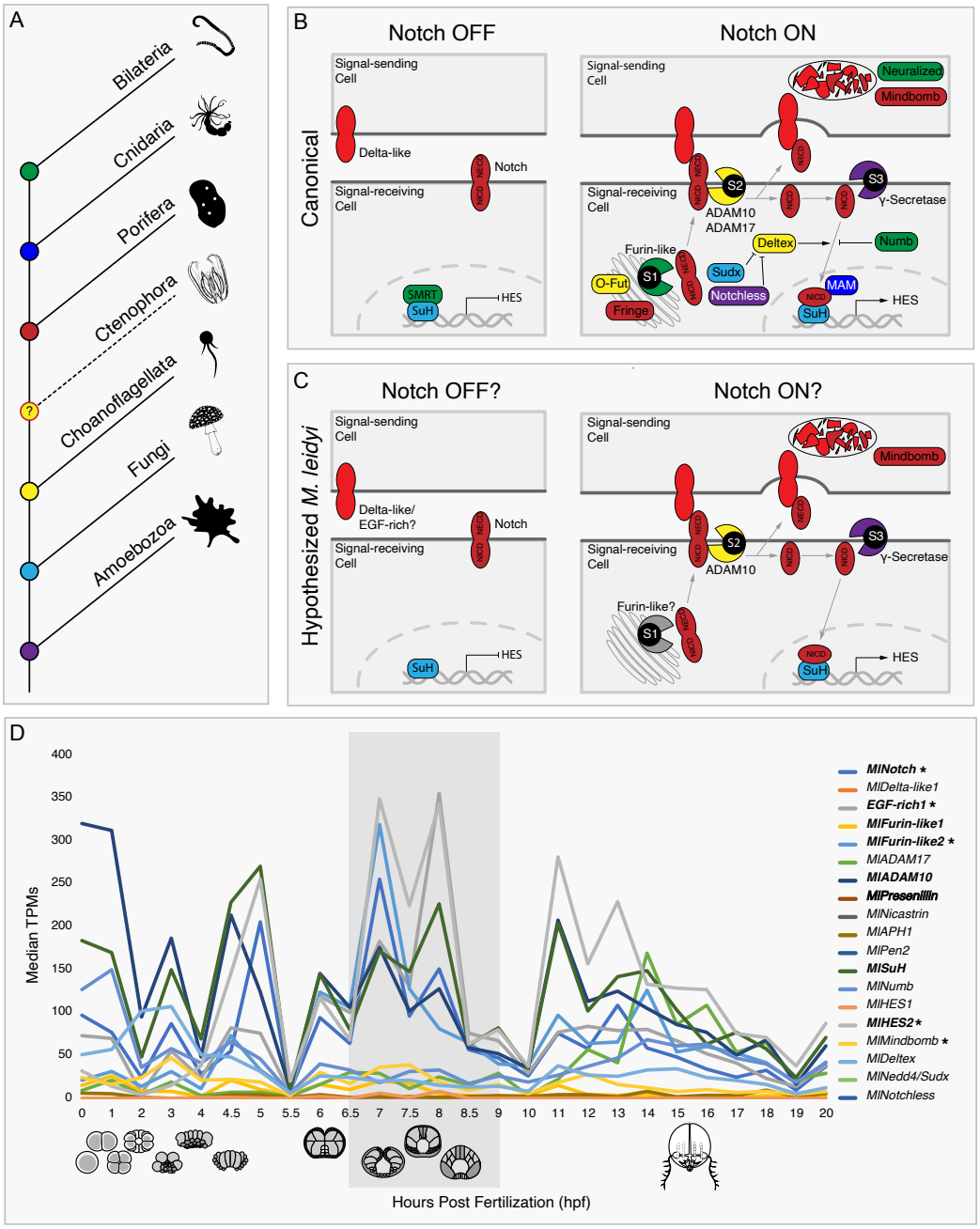

Figure 1. The canonical *Notch* signaling pathway emerged in Metazoan lineages. A) Simple phylogeny depicting when molecular components of the canonical *Notch* pathway evolved. B) Cell diagram of canonical *Notch* pathway in bilaterians, with components color-matched to A) when they are believed to have first emerged. C) Hypothetical cell diagram of components of the putative canonical Notch pathway encoded in the *Mnemiopsis leidyi* genome. D) Developmental RNA-seq of putative canonical *Notch* pathway genes[37]. Bolded genes in the key represent genes expressed during the developmental peak shaded in gray. * = previously unreported genes.

85

86 ***M. leidyi genome encodes many canonical Notch components with characteristic PFAM domains***

87 Many components of the canonical *Notch* pathway are definitively encoded in the genome of the
88 ctenophore *Mnemiopsis leidyi*[18], although these characterizations have been limited to an absent/present
89 dichotomy that assumed that missing components or diagnostic domains of putative *Notch* genes equated
90 non-functionality. However, if these putative canonical components are expressed in the same or adjacent
91 cells at the same time, they could ostensibly behave as a rudimentary pathway (compare Figure 1B to
92 Figure 1C). We therefore examined the cellular and developmental context in which these components are
93 expressed to test the hypothesis that canonical *Notch* components are expressed in shared domains during
94 early ctenophore development and function as a primitive pathway.

95

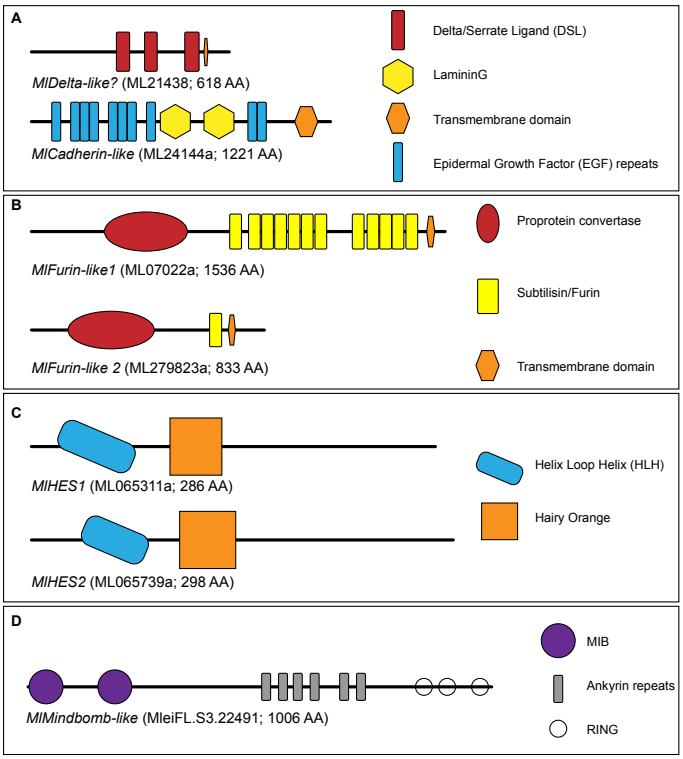

96

97 Figure S1. Domain architectures of proteins implicated in the canonical *Notch* pathway. A) Candidate
98 ligands, *MlDelta-like* and *MlCad-like*. B) Putative S2 proteases, *MlFurin-like1* and *MlFurin-like2*. C)
99 Hairy-Enhancer of Split orthologs, *MlHES1* and *MlHES2*. D) E3 ubiquitin ligase, *MlMindbomb-like.*

100

101 We first confirmed that these ctenophore *Notch* components contain all of their characteristic
102 PFAM domains. We conducted independent BLAST searches of canonical *Notch* components against the
103 *M. leidyi* genome and confirmed hits with reciprocal BLAST and PFAM analysis. Upon examination of
104 the reported *MlDelta-like* (ML21438a) gene, we were able to identify the delta-serrate ligand (DSL)
105 PFAM domains previously reported missing (see Figure S1A and File S1). However, reciprocal BLAST
106 searches did not result in any hit with matching PFAM domains, leading us to conclude that this hit was
107 an error in the genome sequencing. Furthermore, BLAST searches of the *Drosophila Delta-like* sequence
108 against the *M. leidyi* genome yielded the gene identified as *MlNotch* (ML128617a) and a gene rich in both
109 EGF repeats and LamininG domains, characteristic of proto-cadherins (ML24144a; see Figure S1A and
110 File S1). Given that these genes lack both DSL and MNNL domains, we do not consider them true *Delta-*
111 *like* proteins. We therefore refer to ML24144a as *MlCadherin-like* (*MlCad-like*). Our searches also
112 revealed that the Furin-like gene previously reported[18] (ML07022a) retains several Furin-like repeats and
113 subtilase domains characteristic of Furin convertases; we therefore refer to this gene as *MlFurin-like1*. We
114 also identified previously unreported orthologs for a second Furin-like convertase (ML279823a; Figure
115 S1B and File S1), a second HES transcription factor (ML065739a; Figure S1C and File S1), and an
116 ortholog of the *Delta-like* regulator *Mindbomb* (MleFL.S3.22491; Figure S1D and File S1). We refer to
117 these genes as *MlFurin-like2*, *MlHES2*, and *MlMindbomb*, respectively.
118 Using existing developmental RNA-seq data from *M. leidyi*[21], we plotted the median transcripts
119 per million (TPMs) of the putative *Notch* components encoded in the genome identified in our
120 independent searches. We noted three apparent peaks of gene expression at approximately 4 hours post
121 fertilization (hpf), 8hpf, and 12hpf (Figure 1D). We opted to focus our gene expression studies on the
122 8hpf timepoint to avoid potential confounds with the maternal-to-zygotic transcriptional transition[22]. The
123 genes expressed in this 8hpf peak correspond to putative components of the core canonical *Notch*
124 pathway: *MlNotch* (receptor), *MlPCad-like* (candidate ligand), *MlFurin-like2* (S1 cleavage), *MlADAM10*
125 (S2 cleavage), *MlPresenilin* (S3 cleavage), *MlSuH* (co-factor), and *MlHES2* (transcriptional target).
126

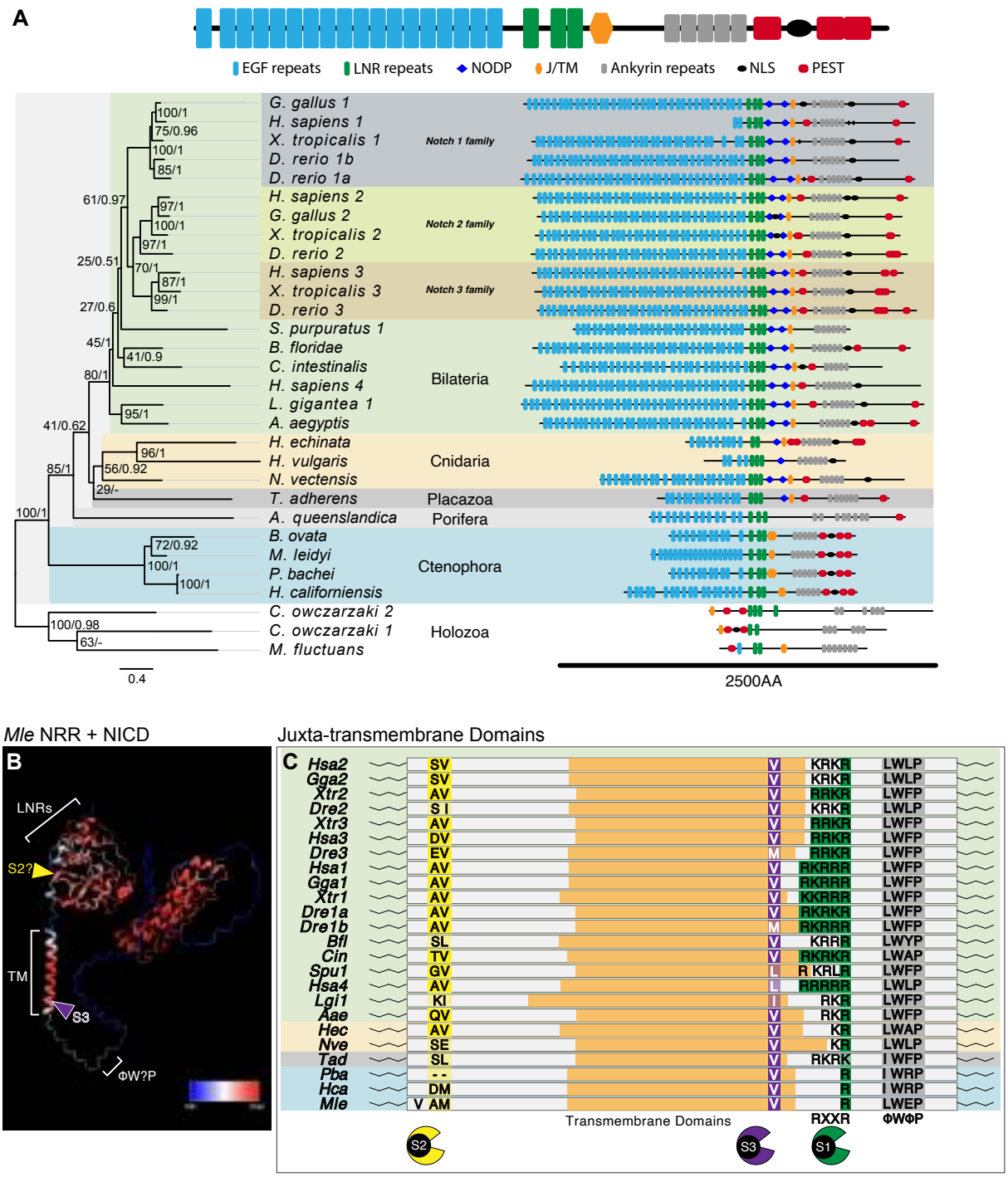

Figure 2 *Notch* domains predate Metazoans. A) Maximum likelihood/Bayesian phylogeny of *Notch* across Metazoa showing conserved *Notch* Intracellular Domains (NICDs). Node labels are Maximum Likelihood / Posterior Probabilities values. B) AlphaFold 3D prediction of *MlNotch* Negative Regulatory Region (NRR) and NICD. C) Basic alignments of *Notch* juxta-transmembrane domains highlighting conserved S1, S2, and S3 cleavage recognition sites. Species in panel C) are color-matched to phyla from panel A).

133

134 ***Notch negative regulatory regions and intracellular domains are highly conserved***

135 We next wanted to evaluate the conserved signaling capacity of the *Notch* receptor by conducting a
136 phylogenetic analysis of *Notch* orthologs across Metaozoa and analyzing their respective PFAM domain
137 architectures and juxta-transmembrane domains (J/TM). Lin-*Notch* Repeats (LNR) and Ankyrin repeats
138 characteristic of *Notch* evolved before the Metazoan lineages. In fact, the LNR and *Notch* Intracellular
139 Domain (NICD) are remarkably conserved across Metazoans, whereas the extracellular Epidermal
140 Growth Factor (EGF) repeats are highly variable (Figure 2A). Our phylogram of *Notch* has strong support
141 placing ctenophore *Notch* proteins at the base of Metazoa, supporting previous supposition that NICD
142 architecture was present in the last common animal ancestor[7]. While each of the predicted ctenophore
143 *Notch* proteins contains conserved nuclear localization signals, we were unable to identify these domains
144 in all of the representative holozoan *Notch-like* proteins.

145 Given that canonical *Notch* signaling activity requires three discrete cleavage events, we wanted
146 to evaluate whether *MlNotch* has conserved regulatory structures and cleavage recognition sites. Our
147 AlphaFold prediction shows that *MlNotch* LNRs cover the extracellular J/TM region in *MlNotch* (Figure
148 2B). Our multiple sequence alignment shows that residues recognized by Furin-like and γ-secretase are
149 highly conserved, whereas the putative S2 cleavage site is poorly conserved (Figure 2C). The minimal
150 Furin-like recognition motif (RXXR) is only observed in bilaterian lineages, although we found a highly
151 conserved Arginine residue aligned in nearly all of the examined sequences. W and P residues of the
152 ΦWΦP motif are also highly conserved. Taken together, these analyses suggest that *MlNotch* may retain
153 signal-transducing capacity independent of S1 or S2 cleavage via Furin-like convertase and ADAM
154 metalloproteases, respectively.

155

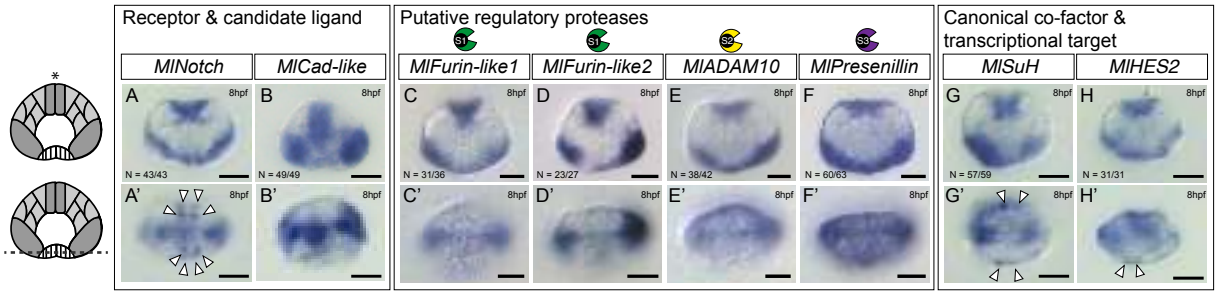

Figure 3. Genes implicated in canonical *Notch* signaling are expressed in developing pharynx and tentacle bulbs at 8hpf. A–A') *MlNotch*. B–B') *MlCad-like*. C–C') *MlFurin-like1*. D–D') *MlFurin-like2*. E–E') *MlADAM10*. F–F') *MlPresenillin*. G–G') *Suppressor-of-Hairless (MlSuH)*. H–H') *MlHairy-Enhancer-of-Split2 (MlHES2)*. * = oral pole. All scalebars = 50µm. White arrowheads indicate distinct patches of expression in aboral cells.

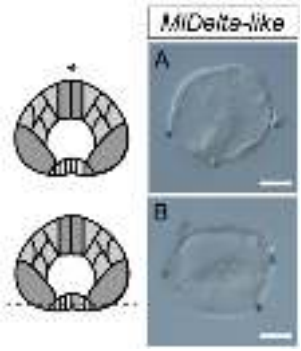

Figure S2. *MlDelta-like* is not detectable 8hpf. A) Lateral view. B) Aboral view. * = oral pole. All scalebars = 50µm.

Putative Notch components share expression domains during late ctenophore embryogenesis

We examined gene expression of *MlNotch* and *MlCad-like* during late embryonic development. *MlNotch* transcripts are broadly expressed at 8hpf in developing pharynx, tentacle bulbs, and aboral organ and in ectodermal cells invaginating at the oral pole (Figure 3A). We also identified a peculiar symmetrical *MlNotch* expression pattern in groups of ectodermal cells at the aboral end of developing embryos (Figure 3A'). *MlCad-like* is expressed in the developing pharynx and tentacle bulbs, similar to *MlNotch* (Figure 3B and Figure 3B'), although we failed to detect clear expression in the aboral end (Figure 3B'). We did not detect expression of the previously identified *MlDelta-like* 8hpf (Figure S2). All four putative protease

genes share broad expression domains at 8hpf in the developing pharynx and tentacle bulbs, although we failed to detect expression of these genes in the aboral end (Figure 3C–3F).

We next examined gene expression of a putative *MlNotch* co-factor (*MlSuH*) and transcriptional target (*MlHES2*). Colorimetric *in situs* of *MlSuH* illustrate a similar expression pattern to *MlNotch* with broad expression domains in the developing pharynx and tentacle bulbs (Figure 3G). We also note patches of *MlSuH* expression in the aboral end of the developing embryo, similar to our observations for *MlNotch* (Figure 3G'). *MlHES2* is expressed in similar domains (Figure 3H and Figure 3H').

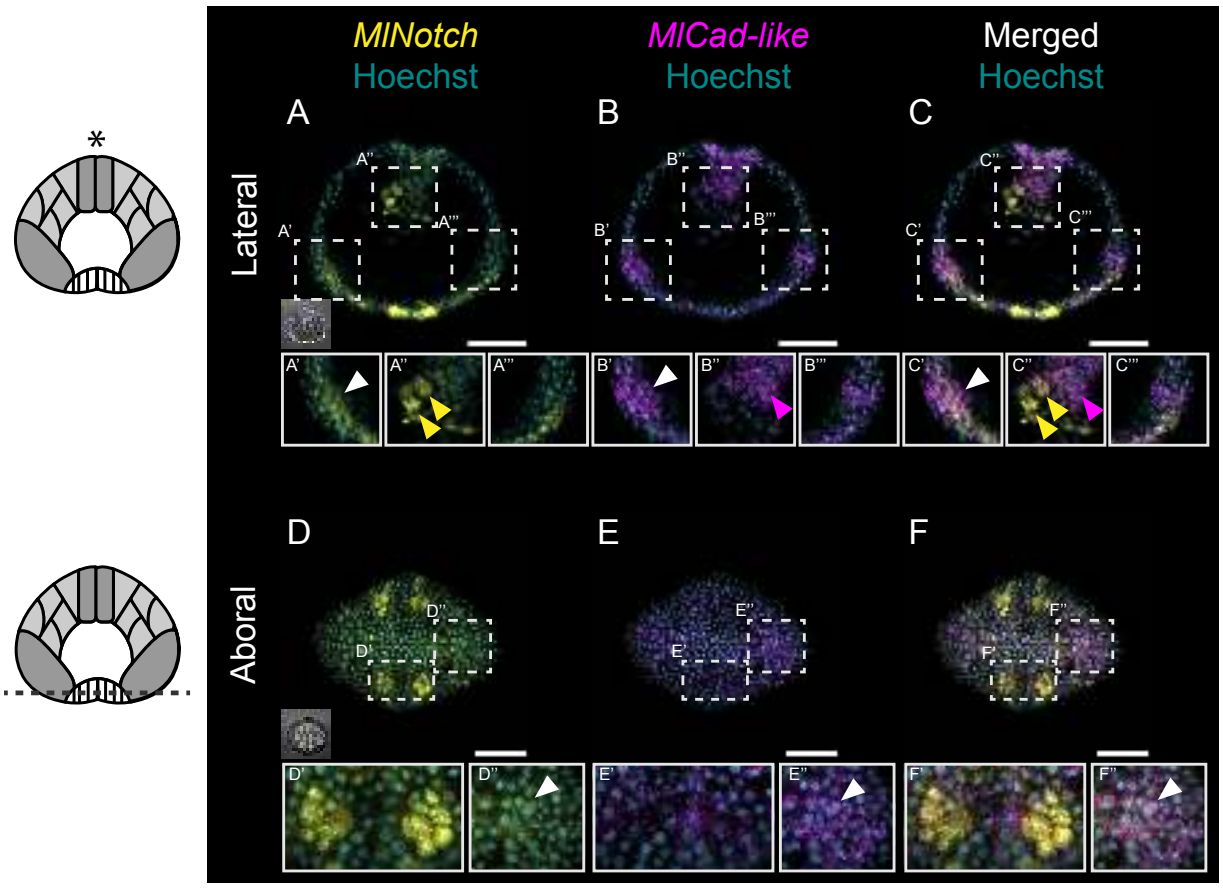

Figure 4. *MlNotch* and *MlCad-like* transcripts are both differentially and co-expressed 8hpf. A–C) Lateral views of *MlNotch* (A), MlCad-like (B), and Merged channels (C). D–F) Aboral views of *MlNotch* (D), *MlCad-like* (E), and Merged channels (F). * = oral pole. All scalebars = 50µm. White arrows indicate cells co-expressing *MlNotch* and *MlCad-like*. Yellow arrows indicate *MlNotch*-positive cells. Magenta arrows indicate *MlCad-like*-positive cells.

190 ***MlNotch and a candidate ligand are expressed in distinct cell populations***

191 To obtain a more cellular resolution of these gene expression patterns, we modified a hybridization chain
192 reaction (HCR™) protocol[23]. We observed weak expression of *MlNotch* in the developing pharynx and
193 tentacle bulbs and identified a strong *MlNotch* signal in distinct patches of cells at the aboral end of 8hpf
194 embryos (Figure 4A). *MlCad-like* signal is most pronounced at the oral pole and developing tentacle
195 bulbs (Figure 4B). While we note apparent regions where *MlNotch* and *MlCad-like* are co-expressed
196 (Figure 4C; see insert 4C'), we also identify differential expression in the developing pharynx and
197 tentacle bulbs (Figure 4C; see inserts 4C''–4C'''). Aboral views confirm the symmetrical nature of
198 *MlNotch* expression in distinct patches of cells, similar to what we observed in our colorimetric *in situs*
199 (Figure 4D; see insert 4D'). *MlCad-like* does not appear to be expressed in the same or neighboring cells
200 in the aboral end of developing embryos (Figure 4E; see insert 4E'). We note regions where *MlNotch* and
201 *MlCad-like* appear to be co-expressed in the ectoderm of the developing tentacle bulbs (Figure 4D–4F;
202 see inserts 4D'', 4E'', and 4F'').

203

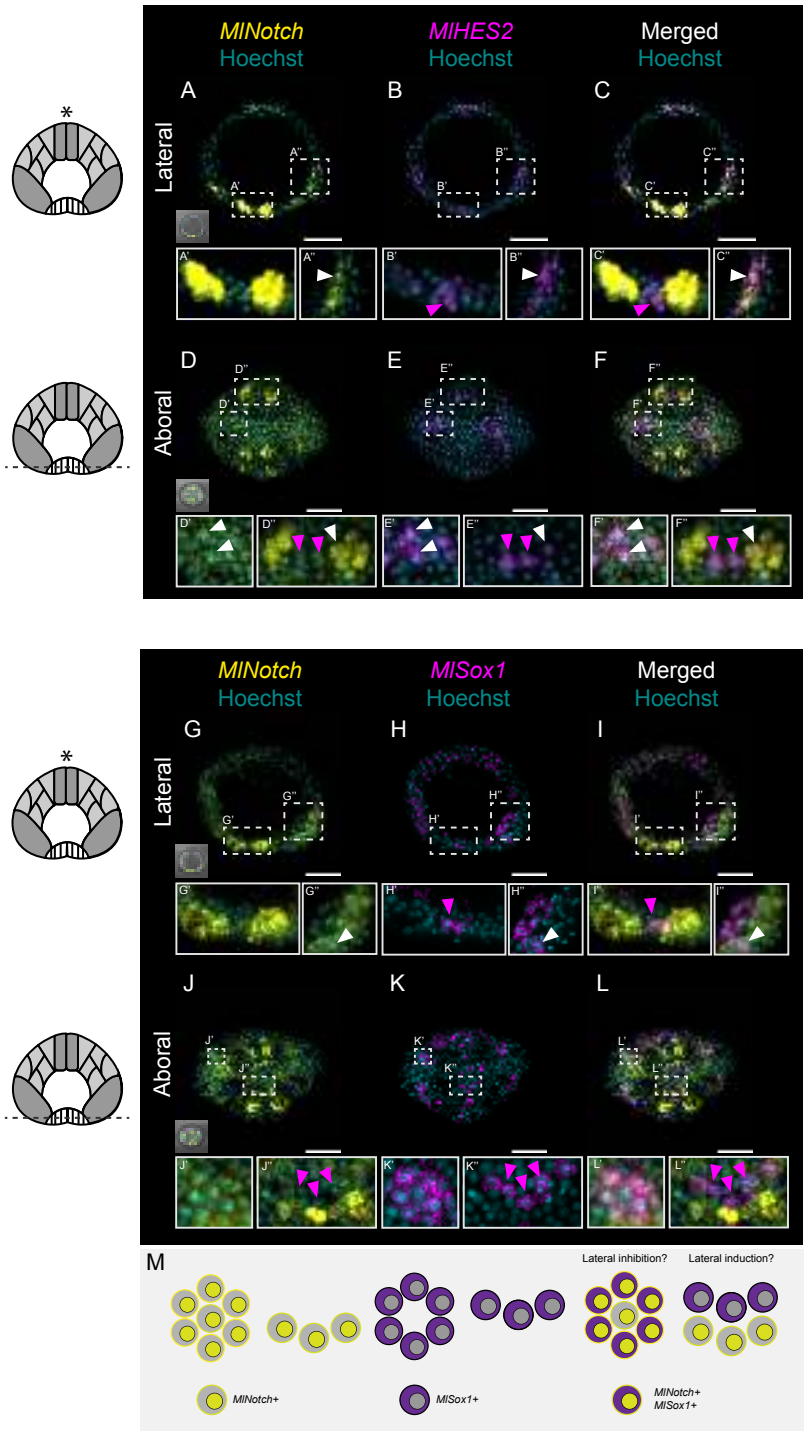

Figure 5. *MlNotch*-positive cells neighbor cells expressing canonical transcriptional targets. A–C) Lateral views of *MlNotch* (A), *MlHES2* (B), and Merged channels (C). D–F) Aboral views of *MlNotch* (D), *MlHES2* (E), and Merged channels (F). G–I) Lateral views of *MlNotch* (G), *MlHES2* (H), and Merged channels (I). Aboral views of *MlNotch* (J), *MlHES2* (K), and Merged channels (L). M) Cartoon schematic representing expression of *MlNotch* relative to *MlSox1* from the panels in J–L. * = oral pole. All scalebars = 50µm. Magenta arrowheads indicate cells expressing *MlHES2* or *MlSox1*, but not *MlNotch*. White arrowheads indicate cells that co-express *MlNotch* and either *MlHES2* or *MlSox1,* respectively.

212

213 ***MlNotch-positive cells co-express canonical transcriptional targets or are found adjacent to cells***

214 ***expressing target transcripts***

215 We next considered expression of *MlNotch* relative to *MlHES2* and *MlSox1*, both canonical

216 transcriptional targets. *MlHES2* shares similar expression domains as *MlCad-like* in the developing

217 tentacle bulbs and pharynx 8hpf, with several cells differentially expressed between *MlNotch*-positive

218 domains in the aboral end (Figure 5A–F). Cells in the developing tentacle bulb appear to co-express

219 *MlNotch* and *MlHES2* transcripts (Figure 5D–F), suggestive of two distinct cell populations or perhaps of

220 a transcriptional transition in cell identity during development.

221 *MlSox1* is a member of the SoxB gene family and has been shown to be expressed in distinctive

222 domains in the aboral end of developing *M. leidyi* embryos with colorimetric *in situ* hybridization[24]. We

223 corroborate that expression pattern here with HCR™ (Figure 5G–L) and show *MlNotch*-positive cells

224 neighboring *MlSox1*-positive cells in the aboral end and developing tentacle bulbs of embryos 8hpf

225 (Figure 5J–L). We also show a previously unidentified ring of *MlSox1*-positive cells medial to an outer

226 ring of *MlNotch*-positive cells near where the apical organ will develop (Figure 5J–L; see inserts 5J",

227 5K", 5L"). These expression patterns are highly reminiscent of classical models of *Notch*-induced lateral

228 inhibition and lateral induction[1,25,26] (see Figure 5M).

229

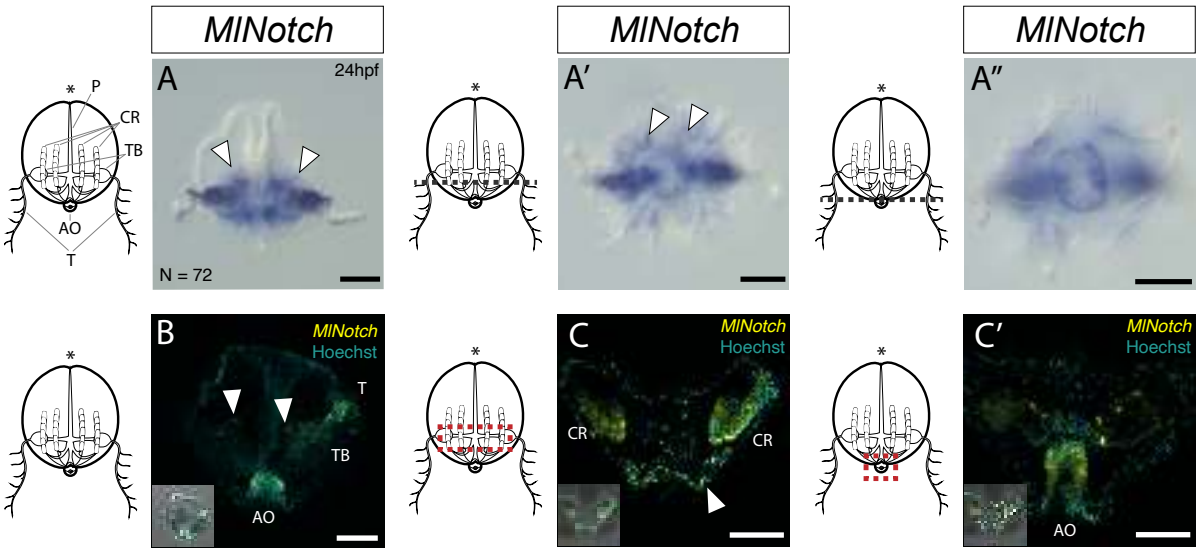

Figure S3. *MlNotch* expression 24hpf. A–A”) Colorimetric ISH of *MlNotch* 24hpf. A) Lateral view showing *MlNotch* expression in mesogleal cells, tentacle bulbs, and floor of the apical organ. A’) Aboral view at the comb row plane showing *MlNotch* expression in presumptive endodermal cells surrounding the comb rows. A”) Aboral view at the plane of the apical organ. B–C’) HCR of *MlNotch* 24hpf. B) Lateral view showing *MlNotch* expression in the floor of the apical organ and in mesogleal cells (see arrowheads). C) Closeup lateral view of *MlNotch*-expressing cells that line the endodermal canals and are sub-adjacent to the comb rows (see arrowhead). C’) Closeup lateral view of *MlNotch*-expressing cells in the floor of the apical organ. * = oral pole. All scalebars = 50µm. P = pharynx, CR = comb rows, TB = tentacle bulb, T = tentacle, AO = apical organ.

MlNotch is expressed in the floor of the apical organ, comb rows, and endodermal canals 24hpf

We were curious to see how *MlNotch* expression and its implied function might change during ctenophore development. Colorimetric *in situ* hybridization shows *MlNotch* expression in gut regions, tentacles, and the floor of the fully developed apical organ of 24h cydippids (Figure S3A–A”). We also note what appears to be cells in the tissue lining endodermal canals (see arrowheads in Figure S3A and 3A’). Aboral views reveal *MlNotch* expression in cells lining the ciliary comb rows (Figure S3A’) and cells that make up the floor of the apical organ (Figure S3A”). HCR™ experiments corroborate our colorimetric *in situs* with strong *MlNotch* signal in neighboring cells of the apical organ (Figure S3B), comb rows and endodermal canals (Figure S3C and Figure S3C’).

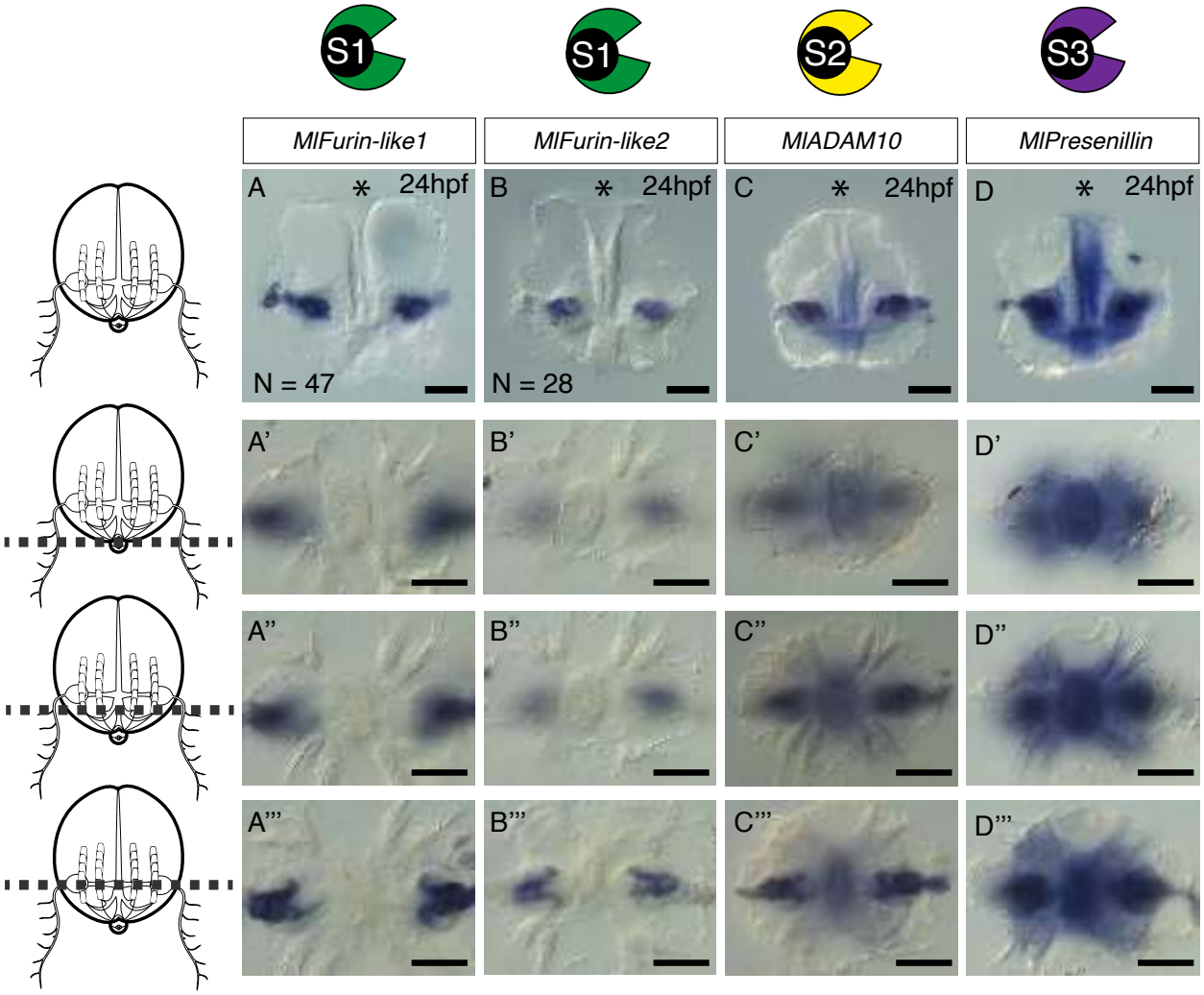

Figure S4. Whole-mount colorimetric *in situ* hybridization of putative genes involved in S1–S3 cleavage. A–A''') *MlFurin-like1* expression show in in lateral view (A), plane of the apical organ (A'), plane of the comb rows (A''), and plane of the tentacle bulbs (A'''). B–B''') *MlFurin-like2* expression show in in lateral view (B), plane of the apical organ (B'), plane of the comb rows (B''), and plane of the tentacle bulbs (B'''). C–C''') *MlADAM10* expression show in in lateral view (C), plane of the apical organ (C'), plane of the comb rows (C''), and plane of the tentacle bulbs (C'''). D–D''') *MlPresenillin* expression show in in lateral view (D), plane of the apical organ (D'), plane of the comb rows (D''), and plane of the tentacle bulbs (D'''). * = oral pole. All scalebars = 50µm.

Putative protease genes share expression domains in the apical organ, tentacle bulbs, and pharynx 24hpf

We evaluated expression patterns of putative S1–S3 protease genes at 24hpf via whole-mount colorimetric *in situ* hybridization. Both *MlFurin-like1* and *MlFurin-like2* are exclusively expressed in

tentacle bulbs in 24h cydippids (Figure S4A–4B; see also Figure S4A''' and 4B'''). *MlADAM10* is also expressed in the tentacle bulbs and pharynx (Figure S4C) with additional expression in the apical organ (Figure S4C'), around the comb rows (Figure 4SC'') and tentacle bulb (Figure S4C'''). *MlPresenillin*, the active subunit of γ-secretase responsible for S3 cleavage, shares similar expression domains in the pharynx, apical organ, and cells surrounding the comb rows (Figure S4D–D'''). These results support conditions in which these genes may be co-expressed to interact in the tentacle bulbs, although they also hint at differential expression — and therefore function — in cells of the apical organ, comb rows, and pharynx.

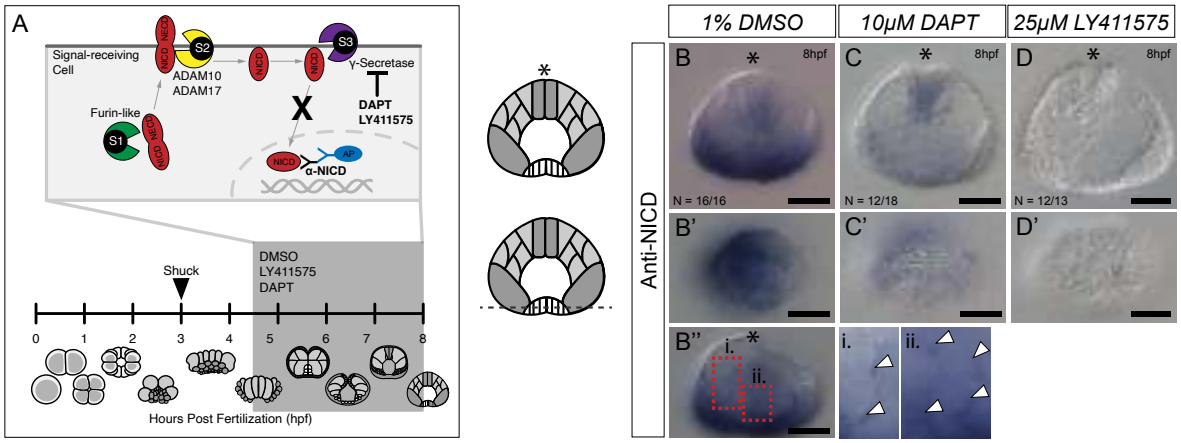

Figure 6. Traditional *Notch* inhibitors reduce expression of *MlNICD* in developing ctenophores. A) Experimental setup of pharmacological inhibition experiments. B–B'') Representative ctenophore embryo incubated in 1% DMSO. B = lateral view, B' = aboral view. B'' shows a lateral view. White arrowheads in i. and ii. point to mesenchymal cells harboring *MlNICD*. C–C') Representative ctenophore embryo incubated in 10μM DAPT. C = lateral view, C' = aboral view. D–D') Representative ctenophore embryo incubated in 25μM LY411575. D = lateral view, D' = aboral view. * = oral pole. All scalebars = 50μm.

Pharmacological inhibition reveals regions of active and inactive MlNotch

To test whether *MlNotch* is cleaved during late ctenophore embryogenesis, we utilized DAPT and LY411575 — both potent γ-secretase inhibitors[27] — combined with an antibody that recognizes cleaved *Notch* (see Figure 6A for experimental setup). We note NICD signal localized to the invaginating pharynx and developing tentacle bulbs (Figure 6B), suggesting that these regions are rich in activated *MlNotch.*

However, we failed to detect signal in the distinctive aboral patches of cells characterized with our colorimetric and HCR *in situs* (Figure 6B'), suggesting that these cell populations are most likely loaded with unprocessed *MlNotch* transcripts or inactive *MlNotch* protein. Mesenchymal cells within the mesoglea also seem to harbor activated *MlNotch* (Figure 6B''; see white arrow heads). Both DAPT- and LY411575-treated embryos show a noticeable decrease in signal within the pharynx and tentacle bulb regions (Figure 6C & Figure 6D). We did not detect any obvious phenotype or loss of cell types in the embryonic or cydippid stages. Furthermore, drug-treated embryos appear to develop into phenotypically normal cydippids. Together, our results are suggestive of a mechanism where "inactive" *MlNotch* regulates a distinct sub-population of cells that, upon cleavage-induced activation, are expressed in mesenchymal cells and cells that contribute to the future tentacle bulb sheath and pharyngeal epithelium.

Discussion

A Notch receptor existed early in the Metazoan divergence and likely retained signaling capacity independent of S1 cleavage

Our bioinformatic structural analysis of the *Notch* juxta-transmembrane domains suggests that *MlNotch* likely does not undergo S1 cleavage. Previous work has identified a Furin-independent function for *Notch* and concluded that this particular role is derived[28,29], although these studies were limited to cell cultures and *Drosophila*. Here, we show that the minimum Furin-like recognition motif (RXXR) in *Notch* was either lost in ctenophore lineages or a bilaterian innovation. Given that our analysis shows that other non-bilaterian Metazoan *Notch* proteins also lack this exact motif, we favor the latter interpretation. This suggests that S1 cleavage and the heterodimerization of the *Notch* receptor could in fact be derived, which in turn would indicate that the Furin-independent function of *Notch* was ancestral.

Similarly, our analysis shows that the S2 cleavage site seems to be highly diverse in non-bilaterian lineages, although *MlNotch* has an LNR domain architecture that may retain a negative regulatory function by covering an as-of-yet unidentified site recognized by another membrane-bound

312 protease (Figure 2B). Choanoflagellates offer a twist in that their *Notch-like* genes also contain structures
313 reminiscent of the negative regulatory regions that, in canonical *Notch* signaling, functions as a cap that
314 covers the S2 sites recognized by ADAM proteinases. In the choanoflagellate *Monosiga brevicolis*,
315 *Notch-like* genes contain an intracellular LNR domain, suggesting that pre-Metazoan *Notch-like* proteins
316 may have been capable of intracellular S2-like cleavages, whereas *M. fluctuans* retains the canonical
317 order of PFAM domains and therefore may have been capable of a more canonical extracellular cleavage.
318 Given that *M. brevicolis* is a more recent lineage, this would suggest that the shuffled *Notch* domains is a
319 derived choanoflagellate characteristic and that the pre-Metazoan *Notch* looked — and may have even
320 functioned — similar to the canonical Metazoan *Notch*.
321
322 ***Developmental and cellular context of MlNotch expression is consistent with models of cell-cell***
323 ***signaling***
324 The putative *Notch* pathway transcripts characterized here all share similar expression domains at the
325 same developmental stage, consistent with what we would expect from components interacting with each
326 other in a functional signaling pathway. The intriguing aboral patches of *MlNotch*-positive cells combined
327 with the data from our pharmacological *Notch* inhibition suggest that these populations are loaded with
328 *MlNotch* transcripts that have not been processed. We hypothesize that these cells are a self-regulating
329 progenitor population characterized by uncleaved — or "inactive" — *MlNotch*. *MlNotch*-positive
330 mesenchymal cells and cells within the developing tentacle bulb and pharynx appear to harbor cleaved —
331 or "active" — *MlNotch*. It is unclear if these active *MlNotch*-positive cells are migrating, but we cannot
332 rule out this possibility. *Notch* signaling has been implicated in coordinating the epithelial-to-
333 mesenchymal transition in cell culture[30] and regulating migratory peripheral glia in *Drosophila*[31], motile
334 cells in zebrafish trunk neural crest[32], and migrating neurons in developing mouse cerebral cortex[33]. To
335 our knowledge, no study has identified a role for *Notch* signaling in regulating migratory cells outside of
336 bilateria. Our results are suggestive of a mechanism where "inactive" *MlNotch* regulates a distinct sub-
337 population of cells that, upon cleavage-induced activation, may be involved in the epithelial-to-

338 mesenchymal transition and the formation of the tentacle bulb sheath and pharyngeal epithelium, pointing
339 to an ancient role for *Notch* regulation of migratory cells. It is unclear what the functions of the other
340 canonical *Notch* pathway genes are in these *Notch*-expressing cells that apparently lack stable cell-cell
341 interactions.

342 As noted previously, the expression of *MlNotch* in relation to putative transcriptional targets,
343 *MlHES2* and *MlSox1*, is highly reminiscent of classical models of lateral inhibition and induction. This
344 result is intriguing, given that *MlSox1* belongs to the SoxB group[34] and *Notch* has been shown to have a
345 conserved role in regulating *Sox* genes. Pharmacological inhibition of *Notch* in *Nematostella vectensis*
346 upregulates *SoxB2* genes[35] while downregulating HES genes[14]. A *Sox*-related gene regulatory network is
347 also moderated by *Notch* in *Hydra vulgaris*[36,37]. *Notch* has also been shown to regulate *Sox* in cephalopod
348 and mouse retinal development[38,39]. *Drosophila* neuroblast formation appears to be gated by a *Notch* and
349 *SoxB* interplay[40]. *SoxB1* coordinates with *NICD* to maintain neural cells in an undifferentiated state in
350 chick embryos[41]. We do not show any clear evidence of *MlNotch* or *MlSox1* promoting neuronal or
351 sensory cell fate in ctenophores, although we do not preclude that possibility. *M. leidyi* embryos develop
352 recognizable neurons by 24hpf, with condensations around the floor of the apical organ by 24hpf[42],
353 precisely where we see *MlNotch* expressed (Figure S3A"). Given that *MlNotch* is expressed well before
354 the first presumptive neuron is differentiated, we hypothesize that this embryonic expression is not
355 promoting terminal neuronal fate, although it could very well be involved in regulating early progenitor
356 cell populations. The localization of *MlNotch* expression at 24hpf in endodermal cells subjacent to comb
357 row cells — where the future gonads will develop — hints at a possible role in promoting primordial
358 germ cell fate.
359

360 ***Pharmacological inhibition of MlNotch points to an as-of-yet unknown mechanism of activation in***
361 ***ctenophores***

362 It is still unclear what activates *MlNotch*. The inability to identify an *MlNotch*-activating ligand has been
363 one of the primary reasons previous reports have concluded that ctenophores do not have a functional

364 *Notch* pathway[9,10,18]. However, the genome of the choanoflagellate species *S. dolichothecata* encodes a
365 protein with MNNL and DSL domains characteristic of *Delta-like*, contrary to previous work suggesting
366 that the *Delta-like* ligand was a Metazoan innovation[7]. Taken together with our ctenophore data, we see at
367 least two possibilities for the emergence of a bonafide *Delta-like* ligand: *Delta-like* could have emerged
368 prior to the Metaozan divergence and was subsequently lost in the ctenophore lineage, or we simply are
369 unable to identify *MlDelta-like* with current methods available to ctenophore researchers.

370 If *Delta-like* was lost in the ctenophore lineage, then *MlNotch* could either function independent
371 of a ligand or it could recognize an as-of-yet unidentified activating ligand. *Notch* activity can occur
372 during *Drosophila* oogenesis independent of ligand activation[43,44]. Perhaps *MlNotch* is capable of such a
373 ligand-independent function. It may even be possible that the ancestral *Notch* could have functioned as a
374 homodimer, acting as both signal and receiver, and *Delta-like* emerged after the ctenophore divergence. It
375 has been hypothesized that the DSL domains characteristic of *Delta-like* proteins shares ancestry with
376 LNR domains of the *Notch* receptor[3]. Furthermore, the DSL domain is extremely similar to EGF domains
377 — perhaps genes rich in EGF architecture could be viable candidates for identifying non-canonical
378 binding partners. The gene hit from our BLAST searches — ML24144a — is an intriguing candidate
379 given its EGF-rich and LamininG-rich extracellular domains, generally characteristic of cadherins.
380 Furthermore, upon re-examination of the genomic architecture surrounding ML24144a, we identified a
381 neighboring gene (ML24143a) that appears to harbor the intracellular domain of a proto-cadherin. It is
382 possible that these two genes are misannotated and are in fact a single proto-cadherin that is co-expressed
383 in cells presumably loaded with active *MlNotch*. This raises the intriguing possibility that the ancestral
384 Metazoan *Notch* interacted with cadherin-like proteins. N-cadherins have been shown to interact with
385 Wnt and *Notch* pathways to regulate neural progenitor cells[45]. Our results are consistent with previous
386 hypotheses that *Notch* signaling could have emerged from a cell adhesion module that predates
387 Metazoa[46]. Our HCR™ data show that *MlNotch* and *MlCad-like* transcripts are co-expressed in distinct
388 cell populations. *Delta-like* and *Jagged-like*, both classical *Notch* ligands, have been shown to be *cis*-
389 activators in synthetic cell cultures[47]. It may be possible that *Notch* communication originated as an

390 autocrine signaling module in single-celled eukaryotes that, due to its association with primitive
391 cadherins, evolved its juxtacrine functions at the base of animal multicellularity.
392 Alternatively, ctenophores could still have a *Delta-like* gene that has evolved such that traditional
393 sequence-based methods are not sensitive enough to identify homologs. Recent work has shown that
394 genes identified as "lineage-specific" may in fact be false-negatives due to the rapid rate in which some
395 genes have evolved such that homologs are unable to be detected[48]. Reasoning that bases homology on
396 sequence similarity or the presence/absence of diagnostic PFAM domains may be similarly flawed. We
397 therefore caution researchers from concluding that specific genes are missing or lineage-specific based on
398 bioinformatic inferences alone, particularly in species where existing genomic and transcriptomic data are
399 prone to errors or mis-annotations.
400
401 **Conclusion**
402 This study paints a more complex picture for *Notch* evolution and its activity during ctenophore
403 development than was previously supposed, laying the groundwork to enrich and expand future studies on
404 the evolution of signaling pathways. We have identified and characterized unreported *Notch* pathway
405 components encoded in the *M. leidyi* genome and clarified the developmental context in which these
406 components are expressed. Our results demonstrate that *MlNotch* expression during ctenophore
407 development is consistent with classical models of cell-cell communication, suggesting that its role as a
408 juxtacrine signal transducer may have evolved at the base of the Metazoan divergence, perhaps through a
409 co-option of a pre-existing cell adhesion module. Furthermore, our results highlight the importance of 1)
410 validating bioinformatic data with *in situ* characterizations before making generalized conclusions and 2)
411 expanding the repertoire of model systems to understand the evolution of developmental signaling
412 pathways. While a relative handful of model systems are powerful to study the basic characteristics of
413 signaling pathways, they offer an extremely limited scope for understanding how these pathways evolved.
414 Despite the unique phylogenetic position and intriguing biology of ctenophores, they remain relatively

415 understudied. *In situ* characterizations of signaling pathways in early-branching Metazoans are crucial for
416 understanding how they evolved their developmental functions.

417

418 **Acknowledgments**

419 This work was supported by the National Science Foundation (NSF grant IOS-1755364), the National
420 Aeronautics and Space Agency (NASA grant 80NSSC18K1067), and The Paul G. Allen Frontiers Group
421 (grant #12970). The authors thank Dr. Alicia Boyd for her valuable comments while drafting this
422 manuscript.

423

424 **Author contributions**

425 Conceptualization, B.F., F.H., and M.Q.M; methodology, B.F., F.H., C.B., and M.Q.M.; validation, B.F.,
426 F.H., and C.B.; formal analysis, B.F., F.H., and C.B.; investigation, B.F., F.H., and C.B.; resources, B.F.,
427 F.H., C.B., J.S., and M.Q.M; data curation, B.F., F.H., and C.B.; writing – original draft, B.F; writing –
428 review and editing, B.F., F.H., C.B., J.S., and M.Q.M.; visualization, B.F., F.H., and C.B.; supervision,
429 F.H. and M.Q.M.; project administration, J.S. and M.Q.M.; funding acquisition, J.S and M.Q.M.

430

431 **Declaration of interests**

432 The authors declare no competing interests.

433

434 **STAR Methods**

435

436 **Resource availability**

437 **Lead contact**

438 Further information and requests for resources and reagents will be fulfilled by the lead contact, Brent
439 Foster (bf400@exeter.ac.uk), or Mark Q. Martindale (mqmartin@ufl.edu).

440

441 **Materials availability**

442 Animals, reagents, and probes generated by this study are available from Mark Q. Martindale
443 (mqmartin@ufl.edu).

444

445 **Data and code availability**

446 This study did not generate any new code.

447

448 **Key resources table**

Reagent or Resource	Source	Identifier
Animal husbandry		
Kreisel		
Grade A Brine Shrimp Eggs	Brine Shrimp Direct	NA
S. Presso, Selco®	Artemia International	NA
Forceps		
Kits		
PGEM-T vector	Promega	Cat #A3600
GeneJET Plasmid Miniprep kit	ThermoFisher	Cat #K0503
MEGAscript SP6	ThermoFisher	Cat #AM1330
MEGAscript T7	ThermoFisher	Cat #AM1334

Fixatives		
ACME	PBS	
	Methanol	
	Glacial Acetic Acid	
	Glycerol	
Rain-X®	Amazon, Inc.	
PFA	Electron Microscopy Sciences	Cat #15710
Gluteraldehyde	Electron Microscopy Sciences	Cat # 16216-10
Methanol	Fisher Scientific	Cat #A4121
In situ* and *HCR probes		

***In situ* hybridization solutions**		
Proteinase K	Invitrogen	Cat# 25530049
Glycine	Sigma Aldrich	Cat# 410225
Triethanolamine	Sigma Aldrich	Cat #90279
Acetic anhydride	Sigma Aldrich	Cat# 320102
Hybridization buffer (with salmon sperm DNA)	Formamide (Sigma Aldrich)	Cat #FX0420
	20X SSC (pH4.5)	NA
	20mg/ml heparin	NA
	100% Tween-20 (ThermoFisher)	Cat # P2287
	20% SDS (ThermoFisher)	Cat# BP166-500
	10mg/ml salmon sperm DNA (Invitrogen)	Cat #AM9680
Hybridization buffer (without salmon sperm DNA)	Formamide (Sigma Aldrich)	Cat #FX0420
	20X SSC (pH4.5)	NA
	20mg/ml heparin	NA
	100% Tween-20 (ThermoFisher)	Cat # P2287
	20% SDS (ThermoFisher)	Cat# BP166-500
2X Saline Sodium-Citrate (SSC), ph7	Sigma Aldrich	Cat# S6639
1X PBS-Tween	100ml 10X PBS	NA
	899ml Milli-Q H_2O	
	1ml Tween-20	

Blocking Buffer	Roche	Cat# 11096176001
Maleic Acid Buffer	6.905g maleic acid	NA
	4.38g NaCl	
	Fill to 1L Milli-Q H_2O	
AP Buffer	100mM NaCl	NA
	100mM Tris-Cl	
	0.5% Tween-20	
	DEPC-H_2O	
AP Buffer with $MgCl_2$	100mM NaCl	NA
	50mM $MgCl_2$	
	100mM Tris-Cl	
	0.5% Tween-20	
	DEPC-H_2O	
NBT (100mg/ml)	Roche	Cat #11383213001
BCIP (50mg/ml)	Roche	Cat #11383223001
AP Developing Buffer	AP Buffer with $MgCl_2$	NA
	NBT (0.33mg/ml)	
	BCIP (0.165mg/ml)	
Antibodies		
Anti-DIG	Roche	Cat #11093274910
Cleaved Notch1 antibody	Cell Signaling Technology	Cat #4147
goat-**α**-Rabbit secondary antibody, AP-conjugated	Invitrogen	Cat #31346
HCR solutions		
HCR™ Probe Hybridization Buffer v3.0	Molecular Instruments, Inc.	NA
HCR™ Probe Wash Buffer v3.0	Molecular Instruments, Inc.	NA
HCR™ Amplifier Buffer v3.0	Molecular Instruments, Inc.	NA
HCR™ Amplifier (3.0): B2-488	Molecular Instruments, Inc.	NA
HCR™ Amplifier (3.0): B1-647	Molecular Instruments, Inc.	NA
HCR™ Amplifier (3.0): B3-647	Molecular Instruments, Inc.	NA

449

450

451 ***Animal collection and husbandry***

452 Adult *Mnemiopsis leidyi* were collected in the Matanzas River estuarine system near St. Augustine and
453 Beverly Beach, FL, and transported to the Whitney Laboratory. Animals were transitioned into 2/3X
454 filtered sea water (FSW) (approximately 25 ppt) and kept in a self-circulating Kreisel system in constant
455 light. Adults were fed several times per day with artemia brine shrimp enriched with S. Presso (Seclo®).
456 Prior to spawning, adult animals were placed in the dark for 3 hours and then transitioned to glass finger
457 bowls. When spawning began, roughly one hour later, embryos were collected in a 30-minute window
458 and allowed to develop until 4 hours post fertilization (hpf), after which the vitelline membrane was
459 manually removed with sharp forceps. Embryos were then allowed to grow up until 8hpf or 24hpf when
460 they were fixed for *in situ* hybridization or HCR™.

461

462 ***Gene Identification and Domain Analysis***

463 *M. leidyi* genes were identified in the *Mnemiopsis* Genome Portal from gene identification numbers[18].
464 Orthology was confirmed via reciprocal BLAST against the NCBI database[49] and PFAM analysis. PFAM
465 architectures were evaluated using a combination of SMART[50] and Prosite[51–53]. Domain significance was
466 determined by E-value (SMART) or score threshold (Prosite) (see Supplementary File 1 for PFAM
467 scores). Juxta-transmembrane domains were confirmed using TMHMM 2.0[54] and the Conserved Domain
468 Search (CDS) from NCBI[55–57] (E-value ≤ 0.01). Nuclear localization signals (NLS) were identified with
469 NL Stradamus[58] (significant posterior probability ≥ 0.6). PEST domains were identified with EPestfind
470 (http://emboss.bioinformatics.nl/cgi-bin/emboss/epestfind; threshold ≥ +5.0 score). Putative S1, S2, and
471 S3 recognition sites were identified from previous publications[59]. *MlNotch* juxta-transmembrane domain
472 (JTMD) was aligned with reported *TaNotch*, *NvNotch*, *HsNotch1, HsNotch4, HsNotch2, HsNotch3,*
473 *DmNotch* JTMDs (see Supplementary File 2).

474

475 ***Phylogeny***

476 Sequences for ctenophores (*Boroe ovata*, *Mnemiopsis leidyi*, and *Hormiphora Califoniensis*) and
477 choanoflagellates (*Capsaspora owczarzaki* and *Mylnosiga fluctuans*) were added to existing
478 alignments[3,16] using MAFFT[60,61] (see Supplementary File 3 for alignments). EGF repeat domains were
479 excluded from the alignments due to their variability across species[3]. Bootstrapped maximum likelihood
480 phylogenies were prepared with RAxMLGUI2.0 using a WAG substitution matrix and executing 500 ML
481 tree inferences and thereafter a thorough ML search. All free model parameters were estimated by
482 RAxML using a gamma model of rate heterogeneity. Bayesian analysis was performed using MrBayes
483 3.2.6 in Geneious[62] using the WAG fixed model and gamma rate variation. Markov Chain Monte Carlo
484 runs of 1,100,000 generations were calculated with trees sampled every 200 generations and with a prior
485 burn-in of 110,000 generations. The best-scoring tree was visualized using FigTree (v1.4.2;
486 http://tree.bio.ed.ac.uk/software/figtree) and annotated in Adobe Illustrator 2022. Juxtatransmembrane
487 alignments were analyzed and visualized with Jalview[63]. AlphaFold predictions were made with
488 ColabFold v1.5.5: AlphaFold2 using MMseqs2[64] (see Supplementary File 3).

489

490 ***Developmental RNAseq for M. leidyi***

491 Developmental RNA-seq data[21] was accessed via the *Mnemiopsis* Genome Portal[18] and plotted in Excel
492 (see Supplementary File 5).

493

494 ***Cloning of in situ probe templates***

495 Probe preparation and colorimetric *in situ* hybridization were conducted as previously described[65], with
496 slight modifications. Gene fragments were ordered with flanking SP7 and T7 promoters from Twist
497 Biosciences, Inc. (see Supplementary File 6 for fragment sequences) and directly PCR amplified for

498 probe synthesis using SP6 and T7 primers. Some genes were amplified from cDNA using gene specific
499 primers. These were then ligated into Promega PGEM-T vector (A3600), then transformed and verified
500 via colony PCR. Plasmids were purified using the ThermoFisher GeneJET Plasmid Miniprep kit
501 (#K0503) and analyzed by Sanger sequencing. DIG-labled RNA probes were transcribed using Invitrogen
502 MEGAscript SP6 (#AM1330) or T7 (#AM1334) kits according to manufacturer directions.

503

504 ***Colorimetric whole-mount in situ hybridization***

505 Whole-mount *in situ* hybridizations were conducted as previously described[65] with slight modifications.
506 Animals were fixed in ACME solution[66] for one hour at room temperature, then subsequently washed in
507 PBS-Tween (see Supplementary File 7 for the detailed protocol). In brief, samples underwent a secondary
508 fixation in 4% PFA and 0.8% glutaraldehyde for five minutes at room temperature, then transitioned into
509 4% PFA solution overnight at 4ºC. The following day, samples were transitioned to 100% methanol and
510 stored at -20ºC. Samples were subjected to Proteinase K digestion and washes in glycine, triethanolamine,
511 and acetic anhydride before proceeding with an overnight pre-hybridization at 63ºC. Probes were
512 hybridized using 1ng/µl concentrations at 63ºC for 24–72 hours. Samples were transitioned into SSC and
513 PBS-Tween solutions and then blocked in Roche Blocking Buffer (Roche, #11096176001) overnight at
514 4ºC. The following day, samples were incubated with DIG-antibody (Sigma, #11093274910) diluted in
515 Roche Blocking Buffer (Roche, #11096176001, 1:5000) overnight at 4ºC. Samples were then washed in
516 PBS-Tween and washed in alkaline phosphatase (AP) developing buffer (1M NaCl, 2M MgCl2, 1M Tris,
517 Tween-20, NBT, BCIP) to develop DIG-labeled probes.

518

519 ***Hybridization chain reaction RNA fluorescence in situ hybridization (HCR RNA-FISH)***

520 HCR probes were made using a customized Python code[67] and ordered through IDT, Inc., and diluted to
521 100nM stock concentration. Animals were fixed at 8hpf using Rain-X® primary fixation[68] for between

522 20–60 minutes at room temperature, transitioned into PBS-Tween and then subjected to an overnight
523 secondary fixation in 4% PFA at 4ºC. Samples were transitioned into 100% methanol and stored at -20ºC
524 until ready for use, after which they were transitioned back into PBS-Tween. We then followed a standard
525 HCR™ RNA-FISH protocol as described previously[23,69,70], with slight modifications (see Supplementary
526 File 8 for the detailed protocol). Samples were washed in HCR™ Probe Hybridization Buffer v3.0
527 (Molecular Instruments, Inc.) and incubated at 37ºC. Probes were diluted to 20nM in HCR™ Probe
528 Hybridization Buffer v3.0 (Molecular Instruments, Inc.) and were allowed to hybridize overnight at 37ºC,
529 then washed with HCR™ Probe Wash Buffer v3.0 (Molecular Instruments, Inc.). Samples were then
530 washed in HCR™ Amplifier Buffer v3.0 (Molecular Instruments, Inc). Hairpins were heated at 95ºC for
531 90 seconds, then allowed to cool to room temperature in the dark before being added to samples and
532 allowed to amplify overnight at room temperature in the dark. Samples were then washed in 5X SSC and
533 counterstained with Hoechst (1:1000).

534

535 ***Imaging***

536 Colorimetric *in situ* samples were mounted in 80% glycerol and imaged on a Zeiss Imager M2. Images
537 were post-processed in Adobe Photoshop 2022. HCR™ samples were mounted in 5X SSC and imaged on
538 a Zeiss 710 laser scanning confocal microscope. Confocal slices and Z-stacks were analyzed in FIJI[71].

539

540 ***Pharmacological Inhibition***

541 Embryos were de-membranated between 3–4hpf, then treated in 10µM DAPT (Sigma, D5942), 25µM
542 LY411575 (Selleck Chemicals, S2714), and 1% DMSO (Sigma, D4540) in 2/3X FSW for approximately
543 4 hours. We then adapted a standard protocol for antibody staining of *Mnemiopsis leidyi* specimens (see
544 Supplementary File 9 for the detailed antibody staining protocol). In brief, embryos were fixed in Rain-
545 X® (200µl per 1ml) for 20 minutes, then washed into PBS-Tween and stored in 4% paraformaldehyde at

4ºC overnight. The following day, embryos were washed 4 times in PBS-Triton, then permeabilized with 4 washes in PBT and blocked in 5% Normal Goat Serum (NGS) for 1 hour at room temperature. Cleaved Notch1 antibody (Cell Signaling Technology, #4147, 1:500) was diluted in 5% NGS and incubated with samples overnight at 4ºC. Embryos were washed 7 times in PBT, then incubated with goat-**α**-Rabbit secondary antibody conjugated with AP (Invitrogen, #31346, 1:3500) and incubated overnight at 4ºC. The specimens were then washed twice in AP developing buffer without $MgCl_2$ (1M NaCl, 1M Tris, Tween-20), then washed twice in AP buffer with $MgCl_2$ (1M NaCl, 2M $MgCl_2$, 1M Tris, Tween-20), then developed in AP buffer with NBT and BCIP.

Supplemental information

References

1. Borggrefe, T., and Oswald, F. (2009). The Notch signaling pathway: Transcriptional regulation at Notch target genes. Cell. Mol. Life Sci. *66*, 1631–1646. https://doi.org/10.1007/s00018-009-8668-7.

2. Sachan, N., Sharma, V., Mutsuddi, M., and Mukherjee, A. (2024). Notch signalling: multifaceted role in development and disease. The FEBS Journal *291*, 3030–3059. https://doi.org/10.1111/febs.16815.

3. Gazave, E., Lapébie, P., Richards, G.S., Brunet, F., Ereskovsky, A.V., Degnan, B.M., Borchiellini, C., Vervoort, M., and Renard, E. (2009). Origin and evolution of the Notch signalling pathway: An overview from eukaryotic genomes. BMC Evolutionary Biology *9*, 1–27. https://doi.org/10.1186/1471-2148-9-249/FIGURES/12.

4. Babonis, L.S., and Martindale, M.Q. (2017). Phylogenetic evidence for the modular evolution of metazoan signalling pathways. Philosophical Transactions of the Royal Society B: Biological Sciences *372*. https://doi.org/10.1098/RSTB.2015.0477.

5. King, N., Westbrook, M.J., Young, S.L., Kuo, A., Abedin, M., Chapman, J., Fairclough, S., Hellsten, U., Isogai, Y., Letunic, I., et al. (2008). The genome of the choanoflagellate Monosiga brevicollis and the origin of metazoans. Nature *451*, 783–788. https://doi.org/10.1038/nature06617.

6. Suga, H., and Ruiz-Trillo, I. (2013). Development of ichthyosporeans sheds light on the origin of metazoan multicellularity. Developmental Biology *377*, 284–292. https://doi.org/10.1016/j.ydbio.2013.01.009.

7. Richter, D.J., Fozouni, P., Eisen, M.B., and King, N. (2018). Gene family innovation, conservation and loss on the animal stem lineage. eLife *7*, e34226. https://doi.org/10.7554/eLife.34226.

8. Lv, Y., Pang, X., Cao, Z., Song, C., Liu, B., Wu, W., and Pang, Q. (2024). Evolution and Function of the Notch Signaling Pathway: An Invertebrate Perspective. IJMS *25*, 3322. https://doi.org/10.3390/ijms25063322.

9. Lövy, A., Kyslík, J., Picard-Sánchez, A., Holzer, A.S., Krejčí, A., and Fiala, I. (2025). The Notch pathway in Metazoa: a comparative analysis across cnidarians and beyond. EvoDevo *16*, 8. https://doi.org/10.1186/s13227-025-00246-6.

10. He, X., Wu, F., Zhang, L., Li, L., and Zhang, G. (2021). Comparative and evolutionary analyses reveal conservation and divergence of the notch pathway in lophotrochozoa. Scientific Reports *11*. https://doi.org/10.1038/s41598-021-90800-8.

11. Richards, G.S., and Degnan, B.M. (2012). The expression of Delta ligands in the sponge Amphimedon queenslandica suggests an ancient role for Notch signaling in metazoan development. EvoDevo *3*, 15. https://doi.org/10.1186/2041-9139-3-15.

12. Richards, G.S., Simionato, E., Perron, M., Adamska, M., Vervoort, M., and Degnan, B.M. (2008). Sponge Genes Provide New Insight into the Evolutionary Origin of the Neurogenic Circuit. Current Biology *18*, 1156–1161. https://doi.org/10.1016/j.cub.2008.06.074.

13. Marlow, H., Roettinger, E., Boekhout, M., and Martindale, M.Q. (2012). Functional roles of Notch signaling in the cnidarian Nematostella vectensis. Developmental Biology *362*, 295–308. https://doi.org/10.1016/J.YDBIO.2011.11.012.

14. Layden, M.J., and Martindale, M.Q. (2014). Non-canonical Notch signaling represents an ancestral mechanism to regulate neural differentiation. EvoDevo *5*, 30. https://doi.org/10.1186/2041-9139-5-30.

15. Haillot, E., Lebedeva, T., Steger, J., Genikhovich, G., Montenegro, J.D., Cole, A.G., and Technau, U. (2024). Notch, β-catenin and MAPK signaling segregate endoderm and mesoderm in the diploblast *Nematostella vectensis*. Preprint, https://doi.org/10.1101/2024.10.29.620801 https://doi.org/10.1101/2024.10.29.620801.

16. Gahan, J.M., Schnitzler, C.E., DuBuc, T.Q., Doonan, L.B., Kanska, J., Gornik, S.G., Barreira, S., Thompson, K., Schiffer, P., Baxevanis, A.D., et al. (2017). Functional studies on the role of Notch signaling in Hydractinia development. Developmental Biology *428*, 224–231. https://doi.org/10.1016/J.YDBIO.2017.06.006.

17. Käsbauer, T., Towb, P., Alexandrova, O., David, C.N., Dall'Armi, E., Staudigl, A., Stiening, B., and Böttger, A. (2007). The Notch signaling pathway in the cnidarian Hydra. Developmental biology *303*, 376–390. https://doi.org/10.1016/J.YDBIO.2006.11.022.

18. Ryan, J.F., Pang, K., Schnitzler, C.E., Nguyen, A.D., Moreland, R.T., Simmons, D.K., Koch, B.J., Francis, W.R., Havlak, P., Smith, S.A., et al. (2013). The genome of the ctenophore Mnemiopsis leidyi and its implications for cell type evolution. Science *342*. https://doi.org/10.1126/SCIENCE.1242592.

19. Moroz, L.L., Kocot, K.M., Citarella, M.R., Dosung, S., Norekian, T.P., Povolotskaya, I.S., Grigorenko, A.P., Dailey, C., Berezikov, E., Buckley, K.M., et al. (2014). The ctenophore genome and the evolutionary origins of neural systems. Nature *510*, 109–114. https://doi.org/10.1038/NATURE13400.

20. Schultz, D.T., Haddock, S.H.D., Bredeson, J.V., Green, R.E., Simakov, O., and Rokhsar, D.S. (2023). Ancient gene linkages support ctenophores as sister to other animals. Nature *618*, 110–117. https://doi.org/10.1038/s41586-023-05936-6.

21. Levin, M., Anavy, L., Cole, A.G., Winter, E., Mostov, N., Khair, S., Senderovich, N., Kovalev, E., Silver, D.H., Feder, M., et al. (2016). The mid-developmental transition and the evolution of animal body plans. Nature *531*, 637–641. https://doi.org/10.1038/nature16994.

22. Davidson, P.L., Koch, B.J., Schnitzler, C.E., Henry, J.Q., Martindale, M.Q., Baxevanis, A.D., and Browne, W.E. (2017). The maternal-zygotic transition and zygotic activation of the *Mnemiopsis leidyi* genome occurs within the first three cleavage cycles. Molecular Reproduction Devel *84*, 1218–1229. https://doi.org/10.1002/mrd.22926.

23. Choi, H.M.T., Schwarzkopf, M., Fornace, M.E., Acharya, A., Artavanis, G., Stegmaier, J., Cunha, A., and Pierce, N.A. (2018). Third-generation *in situ* hybridization chain reaction: multiplexed, quantitative, sensitive, versatile, robust. Development *145*, dev165753. https://doi.org/10.1242/dev.165753.

24. Schnitzler, C.E., Simmons, D.K., Pang, K., Martindale, M.Q., and Baxevanis, A.D. (2014). Expression of multiple Sox genes through embryonic development in the ctenophore Mnemiopsis leidyi is spatially restricted to zones of cell proliferation. EvoDevo *5*. https://doi.org/10.1186/2041-9139-5-15.

25. Sjöqvist, M., and Andersson, E.R. (2019). Do as I say, Not(ch) as I do: Lateral control of cell fate. Developmental Biology *447*, 58–70. https://doi.org/10.1016/j.ydbio.2017.09.032.

26. Bray, S.J., and Bigas, A. (2025). Modes of Notch signalling in development and disease. Nat Rev Mol Cell Biol *26*, 522–537. https://doi.org/10.1038/s41580-025-00835-2.

27. Morohashi, Y., Kan, T., Tominari, Y., Fuwa, H., Okamura, Y., Watanabe, N., Sato, C., Natsugari, H., Fukuyama, T., Iwatsubo, T., et al. (2006). C-terminal Fragment of Presenilin Is the Molecular Target of a Dipeptidic γ-Secretase-specific Inhibitor DAPT (N-[N-(3,5-Difluorophenacetyl)-L-alanyl]-S-phenylglycine t-Butyl Ester). Journal of Biological Chemistry *281*, 14670–14676. https://doi.org/10.1074/jbc.M513012200.

28. Kidd, S., and Lieber, T. (2002). Furin cleavage is not a requirement for Drosophila Notch function. Mechanisms of Development *115*, 41–51. https://doi.org/10.1016/S0925-4773(02)00120-X.

29. Bush, G., diSibio, G., Miyamoto, A., Denault, J.-B., Leduc, R., and Weinmaster, G. (2001). Ligand-Induced Signaling in the Absence of Furin Processing of Notch1. Developmental Biology *229*, 494–502. https://doi.org/10.1006/dbio.2000.9992.

30. Zavadil, J., Cermak, L., Soto-Nieves, N., and Böttinger, E.P. (2004). Integration of TGF-β/Smad and Jagged1/Notch signalling in epithelial-to-mesenchymal transition. EMBO J *23*, 1155–1165. https://doi.org/10.1038/sj.emboj.7600069.

31. Edenfeld, G., Altenhein, B., Zierau, A., Cleppien, D., Krukkert, K., Technau, G., and Klämbt, C. (2007). Notch and Numb are required for normal migration of peripheral glia in Drosophila. Developmental Biology *301*, 27–37. https://doi.org/10.1016/j.ydbio.2006.11.013.

32. Alhashem, Z., Feldner-Busztin, D., Revell, C., Alvarez-Garcillan Portillo, M., Camargo-Sosa, K., Richardson, J., Rocha, M., Gauert, A., Corbeaux, T., Milanetto, M., et al. (2022). Notch controls the cell cycle to define leader versus follower identities during collective cell migration. eLife *11*, e73550. https://doi.org/10.7554/eLife.73550.

33. Hashimoto-Torii, K., Torii, M., Sarkisian, M.R., Bartley, C.M., Shen, J., Radtke, F., Gridley, T., Šestan, N., and Rakic, P. (2008). Interaction between Reelin and Notch Signaling Regulates Neuronal Migration in the Cerebral Cortex. Neuron *60*, 273–284. https://doi.org/10.1016/j.neuron.2008.09.026.

34. Reitzel, A.M., Pang, K., and Martindale, M.Q. (2016). Developmental expression of "germline"- and "sex determination"-related genes in the ctenophore Mnemiopsis leidyi. EvoDevo *7*. https://doi.org/10.1186/S13227-016-0051-9.

35. Richards, G.S., and Rentzsch, F. (2015). Regulation of Nematostella neural progenitors by SoxB, Notch and bHLH genes. Development (Cambridge, England) *142*, 3332. https://doi.org/10.1242/DEV.123745.

36. Moneer, J., Siebert, S., Krebs, S., Cazet, J., Prexl, A., Pan, Q., Juliano, C., and Böttger, A. (2021). Differential gene regulation in DAPT-treated Hydra reveals candidate direct Notch signalling targets. Journal of cell science *134*. https://doi.org/10.1242/jcs.258768.

37. Steichele, M., Sauermann, L., Pan, Q., Moneer, J., De La Porte, A., Heß, M., Mercker, M., Strube, C., Flaswinkel, H., Jenewein, M., et al. (2025). Notch signaling mediates between two pattern-forming processes during head regeneration in *Hydra*. Life Sci. Alliance *8*, e202403054. https://doi.org/10.26508/lsa.202403054.

38. Koenig, K.M., Sun, P., Meyer, E., and Gross, J.M. (2016). Eye development and photoreceptor differentiation in the cephalopod *Doryteuthis pealeii*. Development, dev.134254. https://doi.org/10.1242/dev.134254.

39. Napoli, F.R., Daly, C.M., Neal, S., McCulloch, K.J., Zaloga, A.R., Liu, A., and Koenig, K.M. (2022). Cephalopod retinal development shows vertebrate-like mechanisms of neurogenesis. Current Biology *32*, 5045-5056.e3. https://doi.org/10.1016/j.cub.2022.10.027.

40. Arefin, B., Parvin, F., Bahrampour, S., Stadler, C.B., and Thor, S. (2019). Drosophila Neuroblast Selection Is Gated by Notch, Snail, SoxB, and EMT Gene Interplay. Cell Reports *29*, 3636-3651.e3. https://doi.org/10.1016/j.celrep.2019.11.038.

41. Holmberg, J., Hansson, E., Malewicz, M., Sandberg, M., Perlmann, T., Lendahl, U., and Muhr, J. (2008). SoxB1 transcription factors and Notch signaling use distinct mechanisms to regulate proneural gene function and neural progenitor differentiation. Development *135*, 1843–1851. https://doi.org/10.1242/dev.020180.

42. Norekian, T.P., and Moroz, L.L. (2021). Development of the nervous system in the early hatching larvae of the ctenophore Mnemiopsis leidyi. Journal of Morphology *282*, 1466–1477. https://doi.org/10.1002/JMOR.21398.

43. Palmer, W.H., and Deng, W.-M. (2015). Ligand-Independent Mechanisms of Notch Activity. Trends in Cell Biology *25*, 697–707. https://doi.org/10.1016/j.tcb.2015.07.010.

693 44. Palmer, W.H., Jia, D., and Deng, W.-M. (2014). Cis-interactions between Notch and its ligands block
694 ligand-independent Notch activity. eLife *3*, e04415. https://doi.org/10.7554/eLife.04415.

695 45. Miyamoto, Y., Sakane, F., and Hashimoto, K. (2015). N-cadherin-based adherens junction regulates
696 the maintenance, proliferation, and differentiation of neural progenitor cells during development. Cell
697 Adhesion & Migration *9*, 183–192. https://doi.org/10.1080/19336918.2015.1005466.

698 46. Murata, A., and Hayashi, S.-I. (2016). Notch-Mediated Cell Adhesion. Biology.
699 https://doi.org/10.3390/biology5010005.

700 47. Nandagopal, N., Santat, L.A., and Elowitz, M.B. (2019). Cis-activation in the Notch signaling
701 pathway. eLife *8*. https://doi.org/10.7554/ELIFE.37880.

702 48. Weisman, C.M., Murray, A.W., and Eddy, S.R. (2020). Many, but not all, lineage-specific genes can
703 be explained by homology detection failure. PLoS Biol *18*, e3000862.
704 https://doi.org/10.1371/journal.pbio.3000862.

705 49. Sayers, E.W., Beck, J., Bolton, E.E., Brister, J.R., Chan, J., Connor, R., Feldgarden, M., Fine, A.M.,
706 Funk, K., Hoffman, J., et al. (2025). Database resources of the National Center for Biotechnology
707 Information in 2025. Nucleic Acids Research *53*, D20–D29. https://doi.org/10.1093/nar/gkae979.

708 50. Letunic, I., Khedkar, S., and Bork, P. (2021). SMART: recent updates, new developments and status
709 in 2020. Nucleic Acids Research *49*, D458–D460. https://doi.org/10.1093/nar/gkaa937.

710 51. Sigrist, C.J.A., De Castro, E., Cerutti, L., Cuche, B.A., Hulo, N., Bridge, A., Bougueleret, L., and
711 Xenarios, I. (2012). New and continuing developments at PROSITE. Nucleic Acids Research *41*,
712 D344–D347. https://doi.org/10.1093/nar/gks1067.

713 52. Sigrist, C.J.A. (2002). PROSITE: A documented database using patterns and profiles as motif
714 descriptors. Briefings in Bioinformatics *3*, 265–274. https://doi.org/10.1093/bib/3.3.265.

715 53. De Castro, E., Sigrist, C.J.A., Gattiker, A., Bulliard, V., Langendijk-Genevaux, P.S., Gasteiger, E.,
716 Bairoch, A., and Hulo, N. (2006). ScanProsite: detection of PROSITE signature matches and
717 ProRule-associated functional and structural residues in proteins. Nucleic Acids Research *34*, W362–
718 W365. https://doi.org/10.1093/nar/gkl124.

719 54. Krogh, A., Larsson, B., Von Heijne, G., and Sonnhammer, E.L.L. (2001). Predicting transmembrane
720 protein topology with a hidden markov model: application to complete genomes11Edited by F.
721 Cohen. Journal of Molecular Biology *305*, 567–580. https://doi.org/10.1006/jmbi.2000.4315.

722 55. Wang, J., Chitsaz, F., Derbyshire, M.K., Gonzales, N.R., Gwadz, M., Lu, S., Marchler, G.H., Song,
723 J.S., Thanki, N., Yamashita, R.A., et al. (2023). The conserved domain database in 2023. Nucleic
724 Acids Research *51*, D384–D388. https://doi.org/10.1093/nar/gkac1096.

725 56. Lu, S., Wang, J., Chitsaz, F., Derbyshire, M.K., Geer, R.C., Gonzales, N.R., Gwadz, M., Hurwitz,
726 D.I., Marchler, G.H., Song, J.S., et al. (2020). CDD/SPARCLE: the conserved domain database in
727 2020. Nucleic Acids Research *48*, D265–D268. https://doi.org/10.1093/nar/gkz991.

728 57. Marchler-Bauer, A., Bo, Y., Han, L., He, J., Lanczycki, C.J., Lu, S., Chitsaz, F., Derbyshire, M.K.,
729 Geer, R.C., Gonzales, N.R., et al. (2017). CDD/SPARCLE: functional classification of proteins via

subfamily domain architectures. Nucleic Acids Res *45*, D200–D203. https://doi.org/10.1093/nar/gkw1129.

58. Nguyen Ba, A.N., Pogoutse, A., Provart, N., and Moses, A.M. (2009). NLStradamus: a simple Hidden Markov Model for nuclear localization signal prediction. BMC Bioinformatics *10*, 202. https://doi.org/10.1186/1471-2105-10-202.

59. Van Tetering, G., and Vooijs, M. (2011). Proteolytic Cleavage of Notch: “HIT and RUN” CMM *11*, 255–269. https://doi.org/10.2174/156652411795677972.

60. Katoh, K. (2002). MAFFT: a novel method for rapid multiple sequence alignment based on fast Fourier transform. Nucleic Acids Research *30*, 3059–3066. https://doi.org/10.1093/nar/gkf436.

61. Katoh, K., and Standley, D.M. (2013). MAFFT Multiple Sequence Alignment Software Version 7: Improvements in Performance and Usability. Molecular Biology and Evolution *30*, 772–780. https://doi.org/10.1093/molbev/mst010.

62. Huelsenbeck, J.P., and Ronquist, F. (2001). MRBAYES: Bayesian inference of phylogenetic trees. Bioinformatics *17*, 754–755. https://doi.org/10.1093/bioinformatics/17.8.754.

63. Waterhouse, A.M., Procter, J.B., Martin, D.M.A., Clamp, M., and Barton, G.J. (2009). Jalview Version 2—a multiple sequence alignment editor and analysis workbench. Bioinformatics *25*, 1189–1191. https://doi.org/10.1093/bioinformatics/btp033.

64. Mirdita, M., Schütze, K., Moriwaki, Y., Heo, L., Ovchinnikov, S., and Steinegger, M. (2022). ColabFold: making protein folding accessible to all. Nat Methods *19*, 679–682. https://doi.org/10.1038/s41592-022-01488-1.

65. Mitchell, D.G., Edgar, A., Mateu, J.R., Ryan, J.F., and Martindale, M.Q. (2024). The ctenophore Mnemiopsis leidyi deploys a rapid injury response dating back to the last common animal ancestor. Commun Biol *7*, 203. https://doi.org/10.1038/s42003-024-05901-7.

66. García-Castro, H., Kenny, N.J., Iglesias, M., Álvarez-Campos, P., Mason, V., Elek, A., Schönauer, A., Sleight, V.A., Neiro, J., Aboobaker, A., et al. (2021). ACME dissociation: a versatile cell fixation-dissociation method for single-cell transcriptomics. Genome Biol *22*, 89. https://doi.org/10.1186/s13059-021-02302-5.

67. Kuehn, E., Clausen, D.S., Null, R.W., Metzger, B.M., Willis, A.D., and Özpolat, B.D. (2022). Segment number threshold determines juvenile onset of germline cluster expansion in *Platynereis dumerilii*. J Exp Zool Pt B *338*, 225–240. https://doi.org/10.1002/jez.b.23100.

68. Mitchell, D.G., Edgar, A., and Martindale, M.Q. (2021). Improved histological fixation of gelatinous marine invertebrates. Front Zool *18*, 29. https://doi.org/10.1186/s12983-021-00414-z.

69. Wang, Y., Zeng, Y., Saka, S.K., Xie, W., Goldaracena, I., Kohman, R.E., Yin, P., and Church, G.M. (2020). Multiplexed in situ protein imaging using DNA-barcoded antibodies with extended hybridization chain reactions. bioRxiv, 274456. https://doi.org/10.1101/274456.

70. Tsuneoka, Y., and Funato, H. (2020). Modified in situ Hybridization Chain Reaction Using Short Hairpin DNAs. Front. Mol. Neurosci. *13*, 75. https://doi.org/10.3389/fnmol.2020.00075.

71. Schindelin, J., Arganda-Carreras, I., Frise, E., Kaynig, V., Longair, M., Pietzsch, T., Preibisch, S., Rueden, C., Saalfeld, S., Schmid, B., et al. (2012). Fiji: an open-source platform for biological-image analysis. Nature Methods 2012 9:7 *9*, 676–682. https://doi.org/10.1038/nmeth.2019.

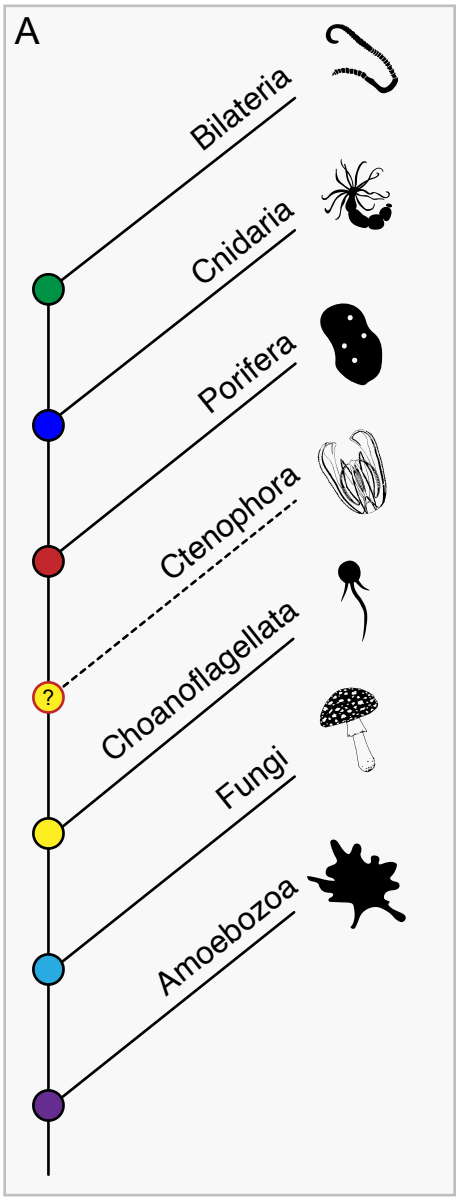
A
Bilateria
Cnidaria
Porifera
Ctenophora
Choanoflagellata
Fungi
Amoebozoa
?

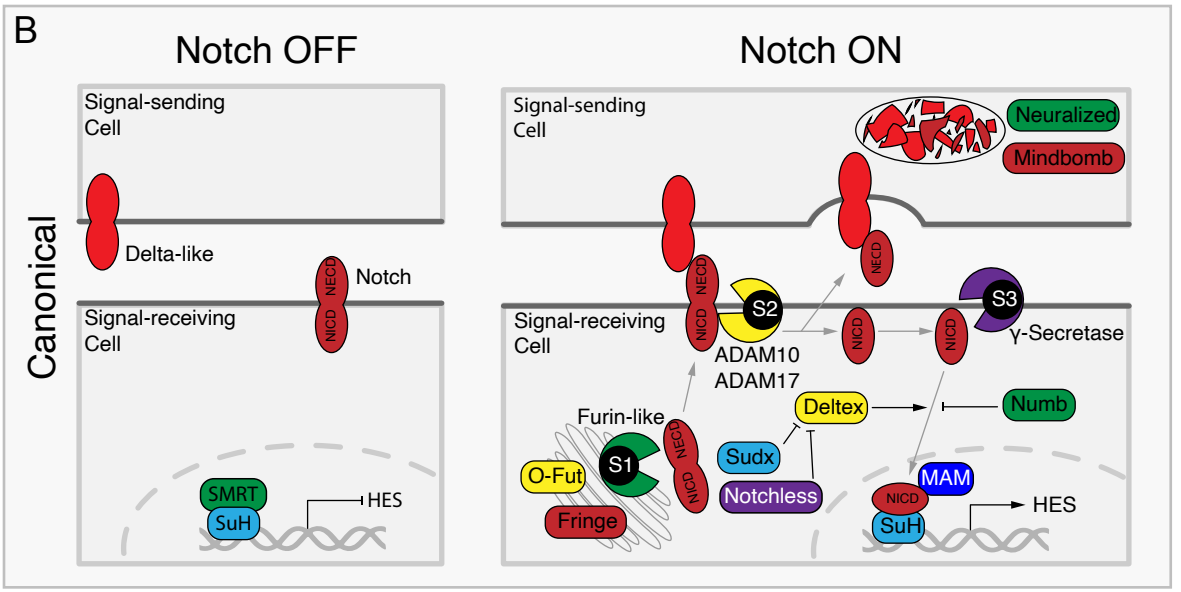
B
Notch OFF
Notch ON
Canonical
Signal-sending Cell
Delta-like
Notch
NECD
NICD
Signal-receiving Cell
SMRT
SuH
HES
Neuralized
Mindbomb
S2
S3
ADAM10
ADAM17
γ-Secretase
Deltex
Numb
Furin-like
S1
O-Fut
Fringe
Sudx
Notchless
MAM

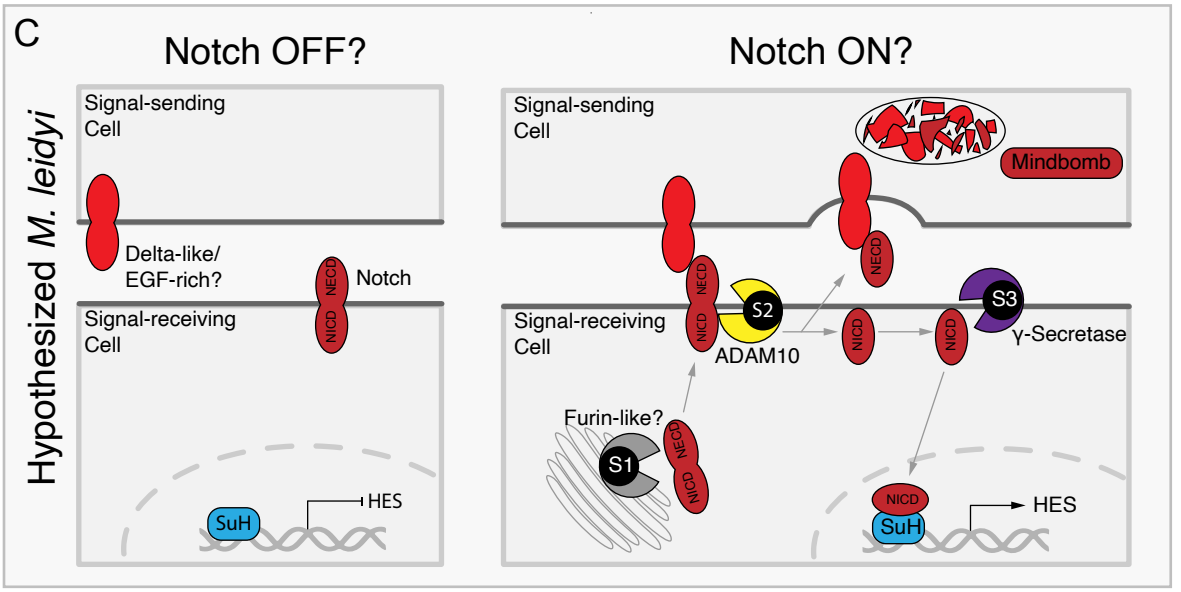
C
Notch OFF?
Notch ON?
Hypothesized M. leidyi
Signal-sending Cell
Delta-like/ EGF-rich?
Notch
NECD
NICD
Signal-receiving Cell
SuH
HES
Mindbomb
S2
S3
ADAM10
γ-Secretase
Furin-like?
S1

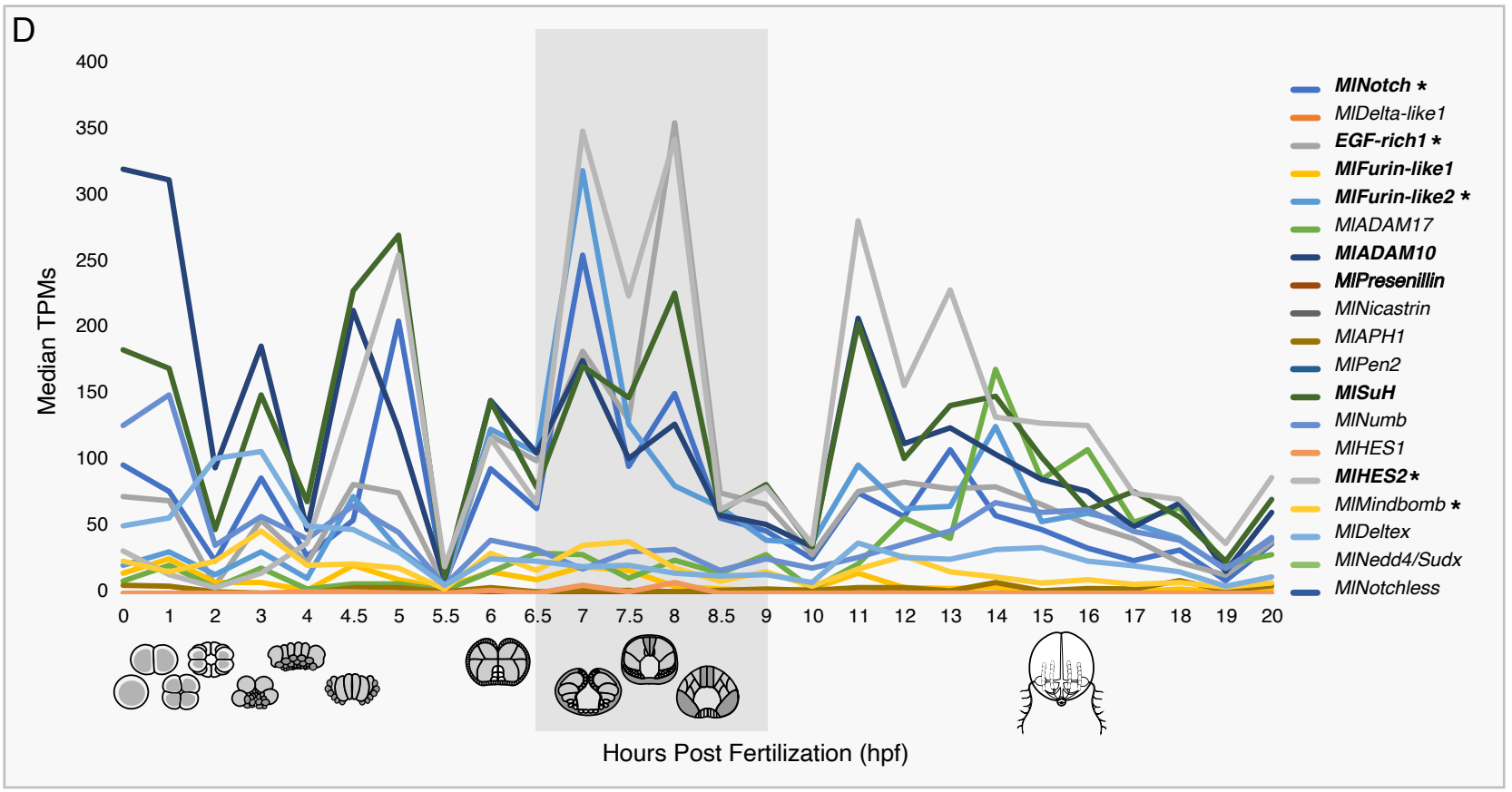
D
Median TPMs
Hours Post Fertilization (hpf)
MlNotch *
MlDelta-like1
EGF-rich1 *
MlFurin-like1
MlFurin-like2 *
MlADAM17
MlADAM10
MlPresenillin
MlNicastrin
MlAPH1
MlPen2
MlSuH
MlNumb
MlHES1
MlHES2 *
MlMindbomb *
MlDeltex
MlNedd4/Sudx
MlNotchless

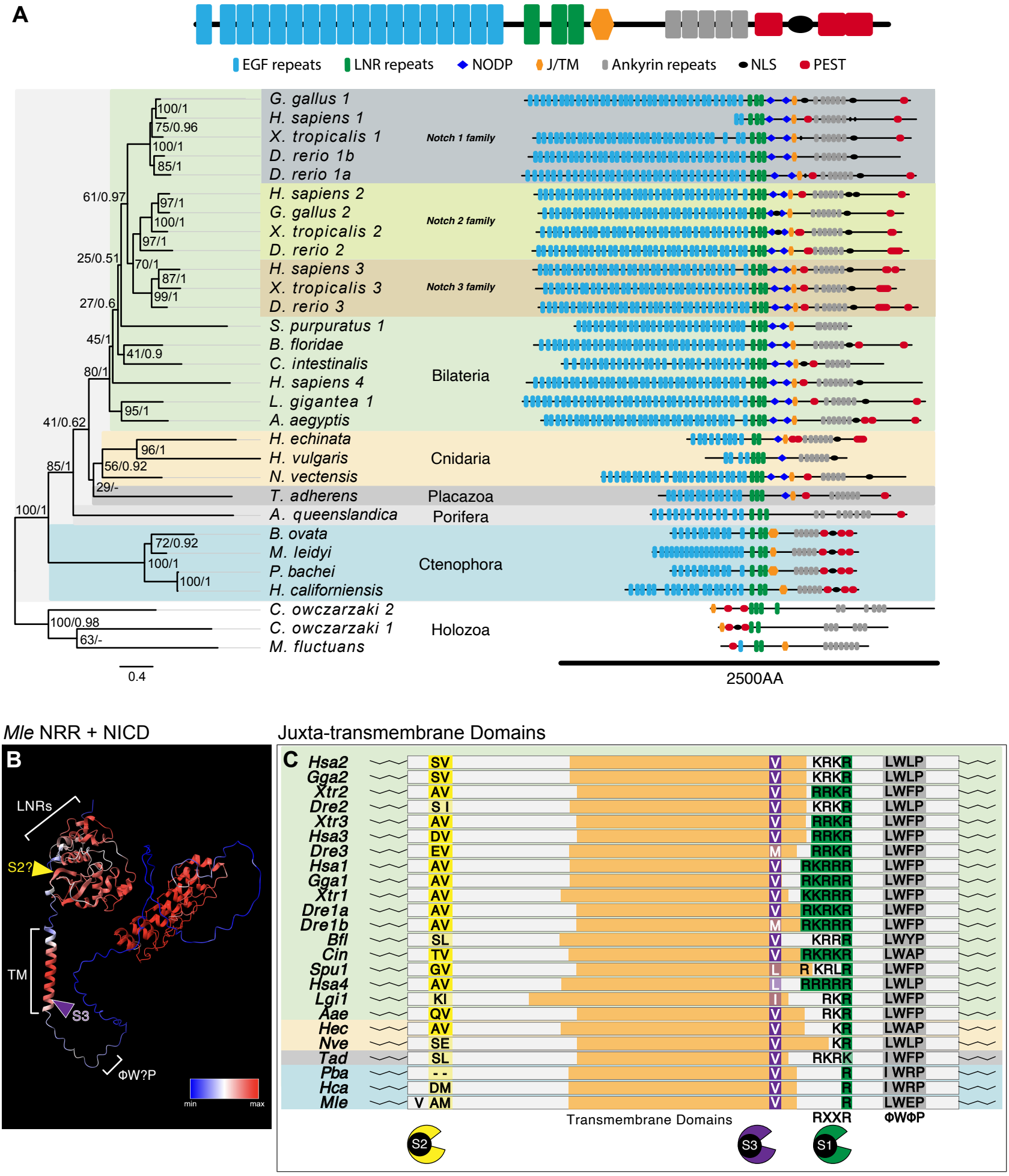
A
EGF repeats
LNR repeats
NODP
J/TM
Ankyrin repeats
NLS
PEST
G. gallus 1
H. sapiens 1
X. tropicalis 1
D. rerio 1b
D. rerio 1a
Notch 1 family
H. sapiens 2
G. gallus 2
X. tropicalis 2
D. rerio 2
Notch 2 family
H. sapiens 3
X. tropicalis 3
D. rerio 3
Notch 3 family
S. purpuratus 1
B. floridae
C. intestinalis
H. sapiens 4
L. gigantea 1
A. aegyptis
Bilateria
H. echinata
H. vulgaris
N. vectensis
Cnidaria
T. adherens
Placazoa
A. queenslandica
Porifera
B. ovata
M. leidyi
P. bachei
H. californiensis
Ctenophora
C. owczarzaki 2
C. owczarzaki 1
M. fluctuans
Holozoa
100/1
75/0.96
100/1
85/1
61/0.97
97/1
100/1
97/1
25/0.51
70/1
87/1
99/1
27/0.6
45/1
41/0.9
80/1
95/1
41/0.62
96/1
56/0.92
85/1
29/-
100/1
72/0.92
100/1
100/1
100/0.98
63/-
0.4
2500AA
Mle NRR + NICD
B
LNRs
S2?
TM
S3
ΦW?P
min
max
Juxta-transmembrane Domains
C
Hsa2 SV V KRKR LWLP
Gga2 SV V KRKR LWLP
Xtr2 AV V RRKR LWFP
Dre2 S I V KRKR LWLP
Xtr3 AV V RRKR LWFP
Hsa3 DV V RRKR LWFP
Dre3 EV M RRKR LWFP
Hsa1 AV V RKRRR LWFP
Gga1 AV V RKRRR LWFP
Xtr1 AV V KKRRR LWFP
Dre1a AV V RKRKR LWFP
Dre1b AV M RKRRR LWFP
Bfl SL V KRRR LWYP
Cin TV V RKRKR LWAP
Spu1 GV L R KRLR LWFP
Hsa4 AV L RRRRR LWLP
Lgi1 KI I RKR LWFP
Aae QV V RKR LWFP
Hec AV V KR LWAP
Nve SE V KR LWLP
Tad SL V RKRK I WFP
Pba - - V R I WRP
Hca DM V R I WRP
Mle V AM V R LWEP
Transmembrane Domains
RXXR
ΦWΦP
S2
S3
S1

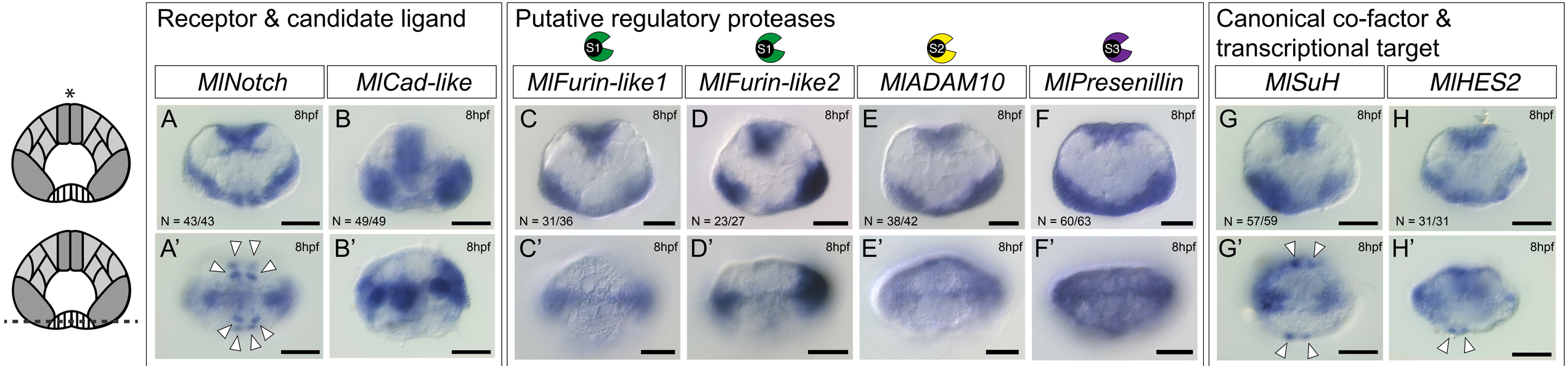
Receptor & candidate ligand
Putative regulatory proteases
Canonical co-factor & transcriptional target
S1
S1
S2
S3
MlNotch
MlCad-like
MlFurin-like1
MlFurin-like2
MlADAM10
MlPresenillin
MlSuH
MlHES2
A
B
C
D
E
F
G
H
A'
B'
C'
D'
E'
F'
G'
H'
8hpf
N = 43/43
N = 49/49
N = 31/36
N = 23/27
N = 38/42
N = 60/63
N = 57/59
N = 31/31
*

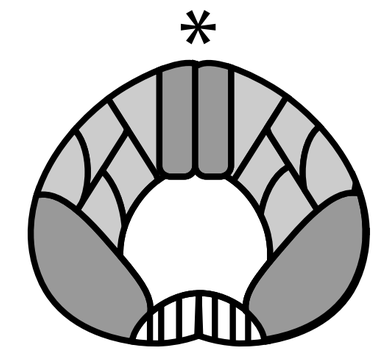
*

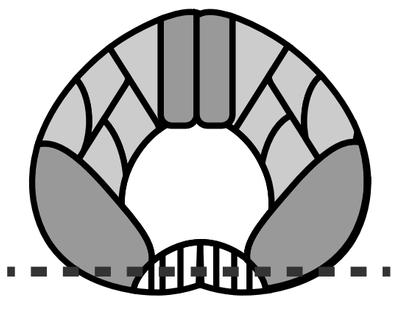

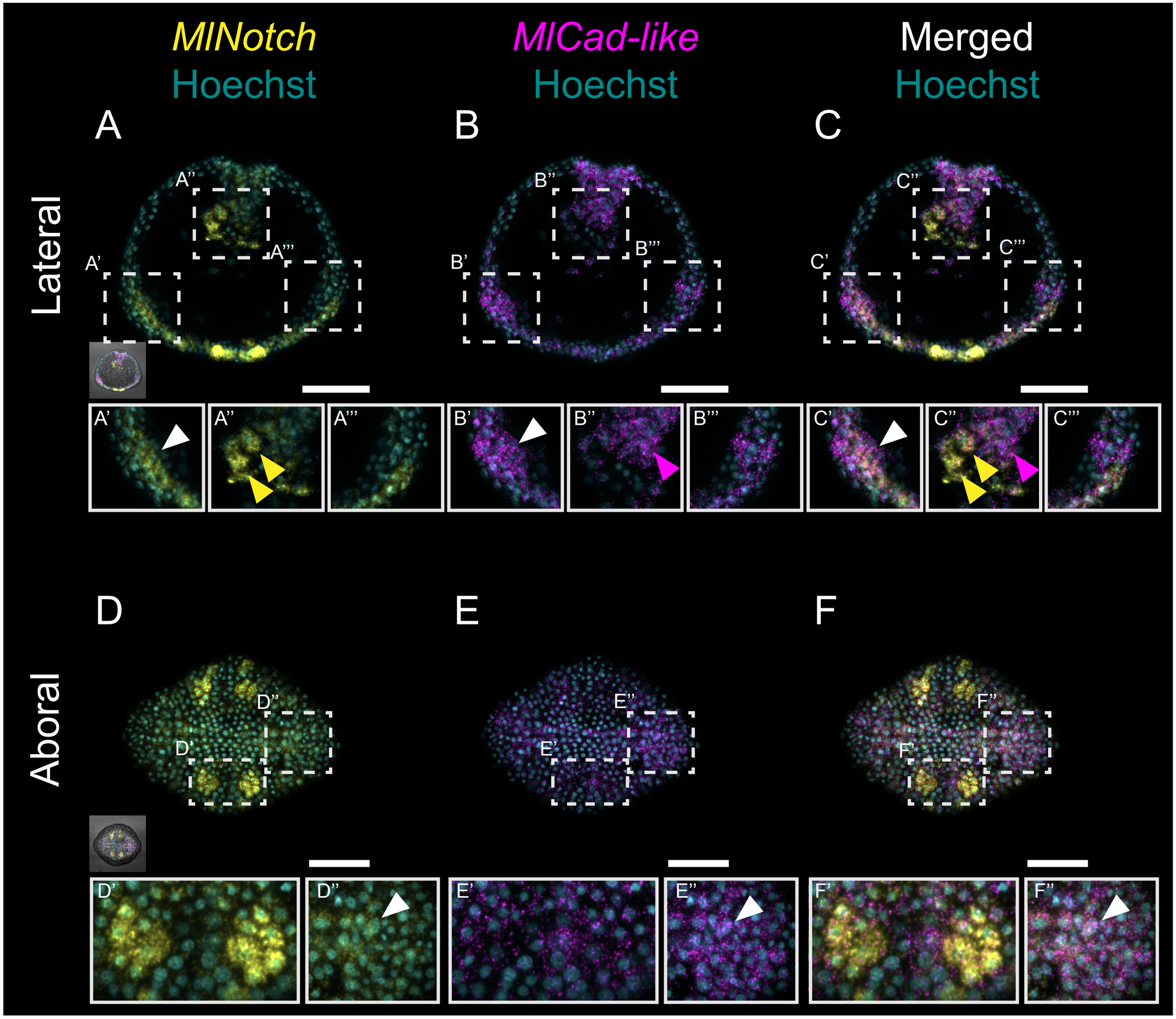
MlNotch
Hoechst
MlCad-like
Hoechst
Merged
Hoechst
A
B
C
Lateral
A'
A''
A'''
B'
B''
B'''
C'
C''
C'''
D
E
F
Aboral
D'
D''
E'
E''
F'
F''

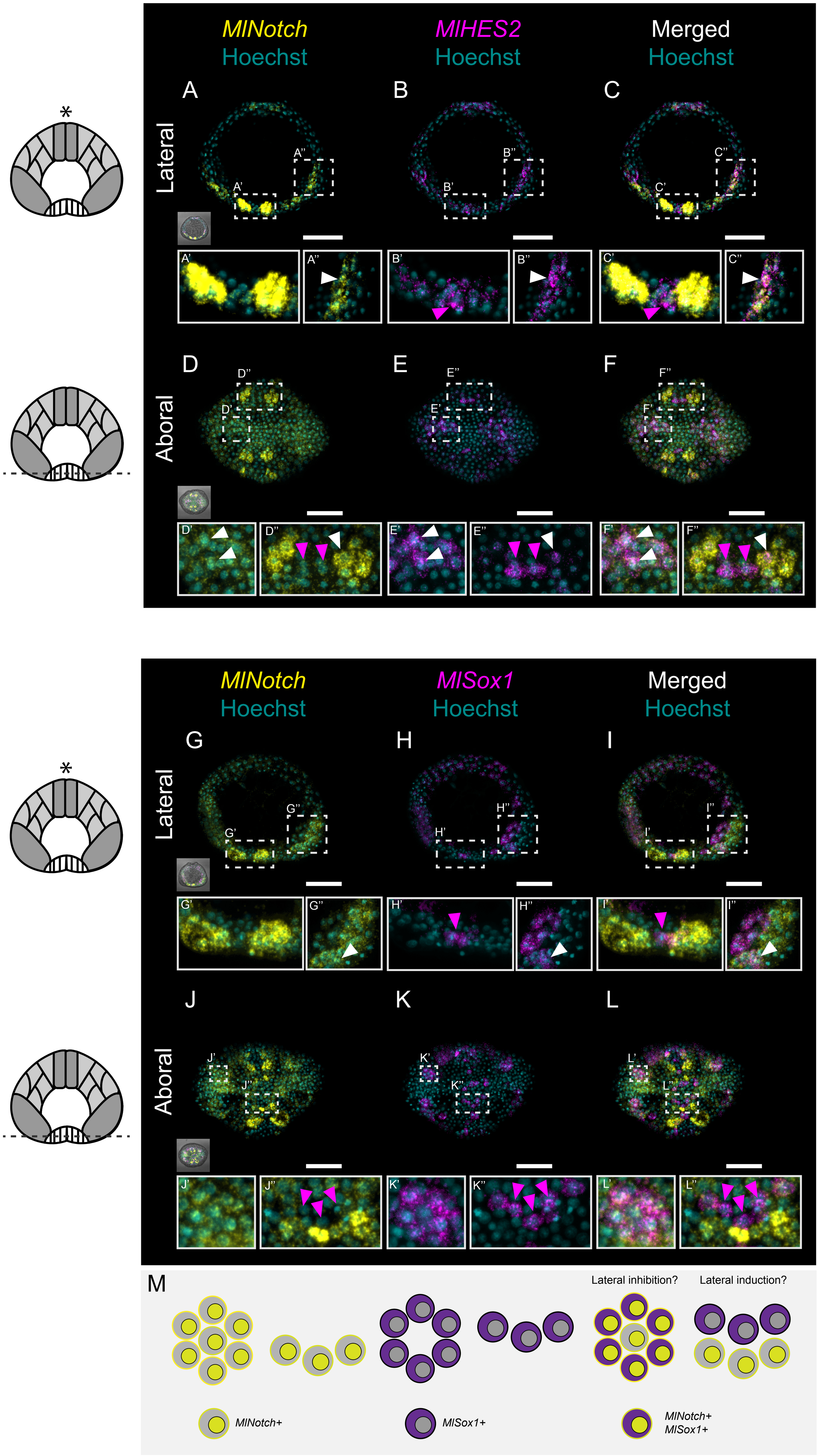
MlNotch
Hoechst
MlHES2
Hoechst
Merged
Hoechst
A
B
C
Lateral
A'
A''
B'
B''
C'
C''
D
E
F
Aboral
D'
D''
E'
E''
F'
F''
MlNotch
Hoechst
MlSox1
Hoechst
Merged
Hoechst
G
H
I
Lateral
G'
G''
H'
H''
I'
I''
J
K
L
Aboral
J'
J''
K'
K''
L'
L''
M
Lateral inhibition?
Lateral induction?
MlNotch+
MlSox1+
MlNotch+
MlSox1+

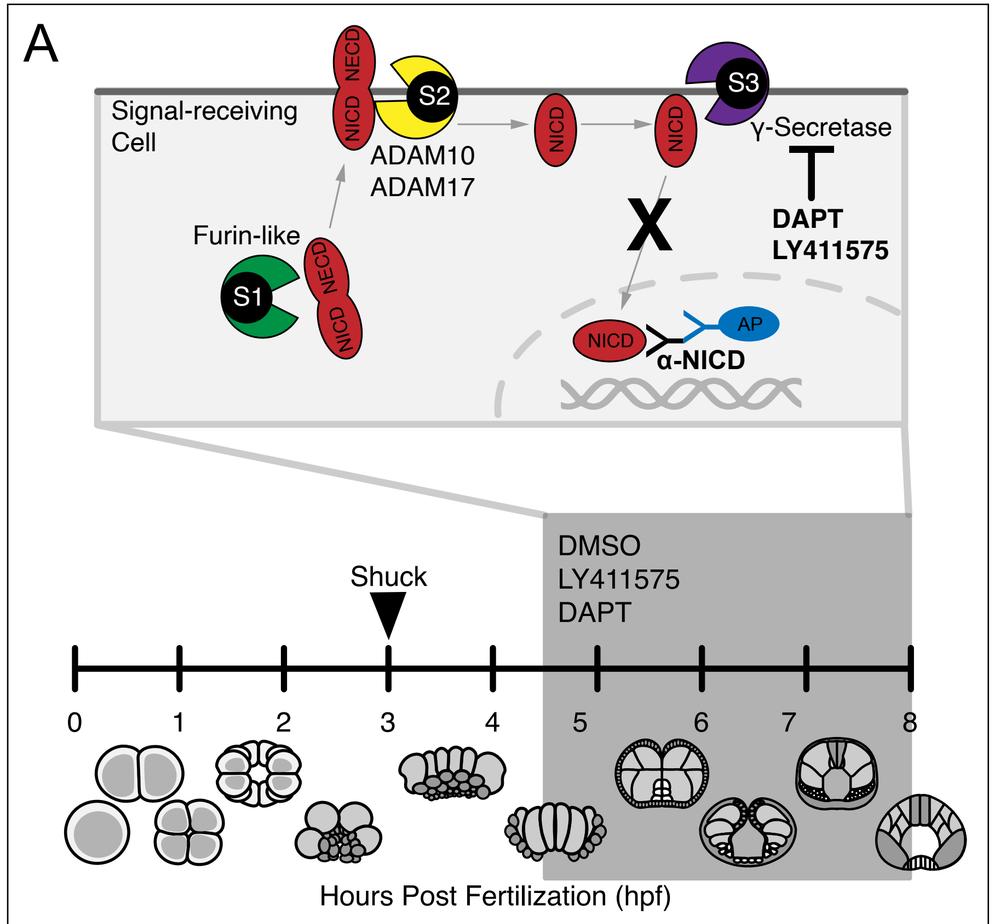
A
Signal-receiving Cell
NICD
NECD
S2
ADAM10
ADAM17
NICD
NICD
S3
γ-Secretase
DAPT
LY411575
X
Furin-like
S1
NICD
NECD
NICD
AP
α-NICD
DMSO
LY411575
DAPT
Shuck
0
1
2
3
4
5
6
7
8
Hours Post Fertilization (hpf)

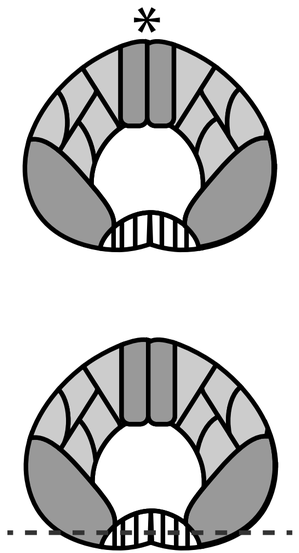
*

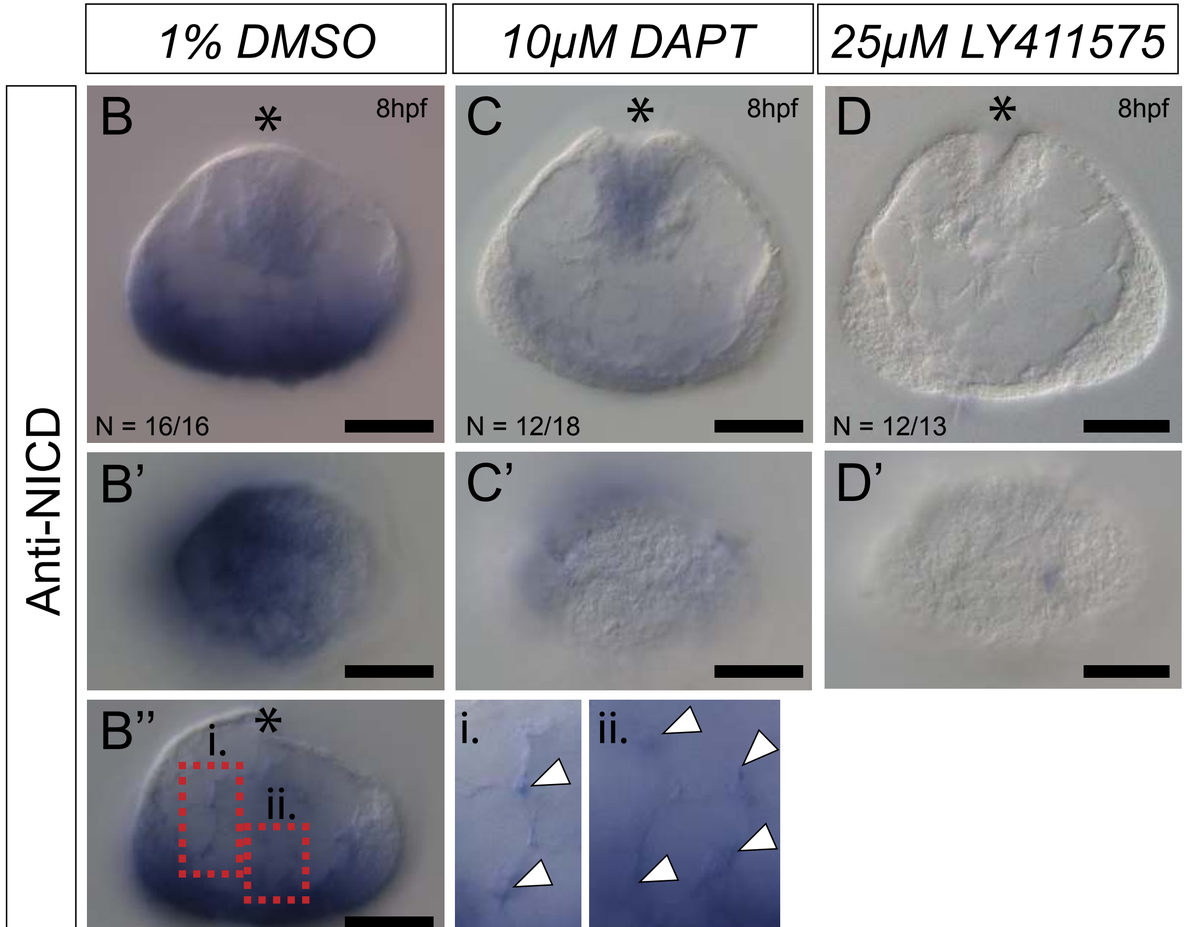
1% DMSO
10μM DAPT
25μM LY411575
Anti-NICD
B
*
8hpf
N = 16/16
C
*
8hpf
N = 12/18
D
*
8hpf
N = 12/13
B'
C'
D'
B''
i.
ii.
*
i.
ii.